Assessing the Role of Organelle-Localized Small Heat Shock Proteins in Stress Tolerance in *Arabidopsis thaliana*

Elana Carleton
Dr. E. Vierling
Honors Thesis

Abstract:

Small heat shock proteins (sHSPs) are a type of molecular chaperone thought to be the first line of defense in the heat stress response. These proteins are ATP-independent molecular chaperones that work with ATP-dependent HSPs in the refolding of aggregated proteins. Despite the presence of sHSPs in virtually every organism, there is limited understanding of how these proteins actually function in vivo, especially the organelle-localized sHSPs found in plants. In *Arabidopsis thaliana*, there are four sHSPs predicted to localize in the mitochondrion and/or chloroplast: HSP23.5, HSP23.6, HSP25.3, and HSP26.5. This project aims to advance the study of the role of these organelle-localized sHSPs in stress tolerance by providing important research tools. One goal includes generating a knockout mutant of chloroplast HSP25.3 to have a complete set of organelle-localized sHSP knockout mutants in the wild-type Colombia background. Wild-type plants have been transformed with a vector carrying specific guide RNAs and the Cas9 protein, have been selected, and can now be tested for an Hsp25.3 mutation. Another goal includes creating an antibody that recognizes HSP23.5 to have a complete set of antibodies to recognize these sHSPs and detect protein expression. A ΔC-Hsp23.5 protein, specific to HSP23.5, has been generated and purified. Currently, an antibody is being produced against this protein. This project also aims to localize each of the four sHSPs using HSP-GFP fusion lines. *A. thaliana* plant lines were screened and localized through microscopy. Additionally, complementation vectors containing the complete wild-type gene of each of the four organelle sHSPs were designed and cloned in order to reintroduce wild-type genes into sHSP mutants. Complementation vectors have been confirmed through colony PCR and restriction digests. Another goal was to generate an assay to test heat stress on plant fertility. Wild-type plants and heat-sensitive null HSP101 mutant plants were heat-stressed and the optimal temperature and treatment that affects seed setting were found. Together, this research provides a better understanding of the four sHSPs and their function in the stress response and allows for further research, including determining the importance of these proteins in plant heat stress tolerance.

Table of Contents

Acknowledgements:

Work was supported in part by **UMass Agriculture Experiment Station – Hatch Project** MAS00566.

Introduction:

Introduction to HSPs and sHSPs

Plants have a conserved response to increased temperatures that protects the plant through the expression of heat shock proteins (HSPs) along with other changes in gene expression and metabolism. The HSPs, though conserved, have diversified in plant species. The most divergent group of HSPs are the small HSPs (sHSPs), which are also a class of molecular chaperones. These sHSPs are independent of ATP and work co-operatively with other ATP-dependent HSPs to refold and prevent irreversible aggregation of other proteins. In plants and other organisms, sHSPs have increased transcription and translation during stress conditions. Some sHSPs can account for over 1% of total leaf or root protein during heat stress conditions, supporting their importance in the stress response (Derocher et al., 1991; Waters et al., 1996). Furthermore, sHSP mRNA and protein levels can increase during different developmental stages across species and in response to different stressors in addition to heat (Basha, 2012).

Classes of sHSPs

There are 11 defined classes of sHSPs in plants. These 11 classes are identified by specific amino acid sequences, motifs, or targeting sequences across species. There are five classes that are cytosolic, known as CI, CII, CIV, CV, and CVI. The 'C' stands for cytosol; these classes do not contain a targeting peptide that would direct their localization to a different cellular compartment. The remaining six classes are localized to specific organelles and have specific targeting peptides (Waters and Vierling, 2020). These are localized to the endoplasmic reticulum, peroxisome, nucleus, mitochondrion, chloroplast, or reported to be dual-localized to the mitochondrion and chloroplast. The most studied sHSPs include the two most abundant

classes of cytosolic sHSPs known as CI and CII. Studies of these two classes has provided the most contribution to understanding the role of sHSPs and to developing the current model of sHSP activity.

sHSP structure

The typical size of sHSPs varies between 12-25 kDa and they are characterized by three domains. They have a divergent N-terminal domain (NTD), a conserved alpha crystallin domain (ACD) of approximately 90 amino acids, and a short C-terminal extension (CTE) (Figure 1). The ACD is a β sheet-rich domain and is the signature domain of the sHSPs (Waters and Vierling, 2020). Studies of sHSPs of *Triticum aestivum* and *Methanocaldococcus janaschii* reveal that the conserved ACD consists of seven to eight strand β-sandwich (Santhanagopalan et al., 2015). Most sHSPs from plants and bacteria assemble into dimers by swapping of β6 strand between proteins. Other sHSPs from metazoans form dimers through an elongated β7 strand. This strand integrates itself anti-parallel to another monomer for the formation of a dimer (Santhanagopalan et al., 2015). The NTD is the most variable domain and contains very few shared motifs across different sHSPs. In plants, chloroplast and mitochondrial sHSPs share the longest NTDs, aside from class V sHSPs, which contain a 30 amino acid motif and an alpha helix motif. Other plant sHSPs, in the cytosol, class I proteins, or in the endoplasmic reticulum share a similar small motif of 10-13 amino acids, while class II cytosolic proteins share a 12 amino acid motif (Waters and Vierling, 2020). Similar to the NTD, the CTE is variable in sequence and is much shorter, averaging 20 or less residues. An I/L-X-I/L motif is the only conserved motif in the CTD (Basha, 2012). Therefore, the NTD and CTD are the regions that account for different overall structures between different sHSPs (Haslbeck and Vierling, 2015). As mentioned before, sHSPs form a basic building block by dimerization through two types of β-strand interaction (Figure 1). These dimers then assemble into oligomers of 12 or more subunits (Waters and Vierling, 2020). The oligomerization occurs by the conserved I/L-X-I/L motif found in the CTD contacting a hydrophobic grove in the ACD (Basha, 2012) and also through interactions of the NTDs.

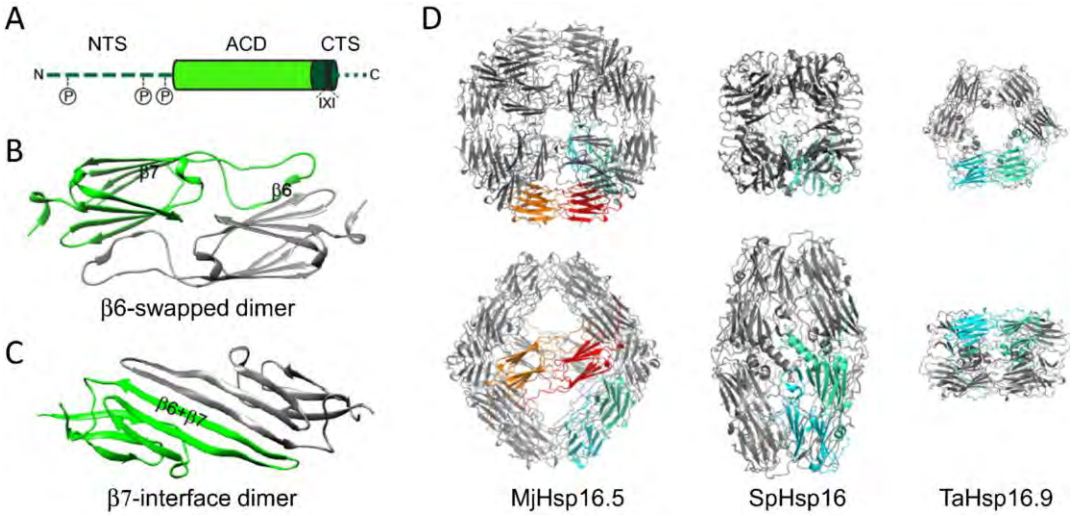

Figure 1: **Structure and domains of sHSPs.** A. Model of the three sHSP domains, including the NTD (here as NTS), ACD, and CTE (here as CTS). B and C represent the interactions of sHSPs to form dimers using either β6 (B) or β7 (C). sHSPs tend to have 12-32 subunits. D. Crystal structures of three different sHSPs from different species; *Methanocaldococcus jannaschii* HSP16.5 (MjHSP16.5) , *Schizosaccharomyces prombe* HSP 16 (SpHSP16), and *Tritium aestivum* HSP16.9 (TaHSP16.9). MjHSP16.5 has 24 subunits, SpHSP16 has 16 subunits, and TaHSP16.9 has 12 subunits. The blue highlight represents a dimer connection. The red and orange highlight is also a dimer connection. From Haslbeck and Vierling, 2015.

Proposed Model for sHSP Chaperone Action

sHSPs can bind to aggregated proteins to aid in the refolding of proteins by ATP-dependent HSPs. A model of the proposed function of sHSPs, displayed in Figure 2, is based on studies of the cytosolic class I sHSPs in plants, as well as studies in cyanobacteria, *E. coli* and humans (Santhanagopalan et al., 2015). In this model, a protein exposed to stress becomes partially unfolded. The sHSPs are mostly in their inactive form, assembled into oligomers, until there is a stress that triggers a response which shifts the equilibrium to the dimeric species, which occurs for example at higher temperatures. The dimers bind to the partially unfolded protein via hydrophobic surfaces. These sHSPs then make the aggregated proteins available to HSP70/DnaK chaperones and protein disaggregase HSP100/ClpB that use ATP to refold the proteins, preventing irreversible aggregation. HSPs can refold protein without the involvement of sHSPs, however, it is proposed the sHSPs increase refolding efficiency (Santhanagopalan et al., 2015). Understanding the role of sHSPs and the specific targeted substrate of these proteins is still limited.

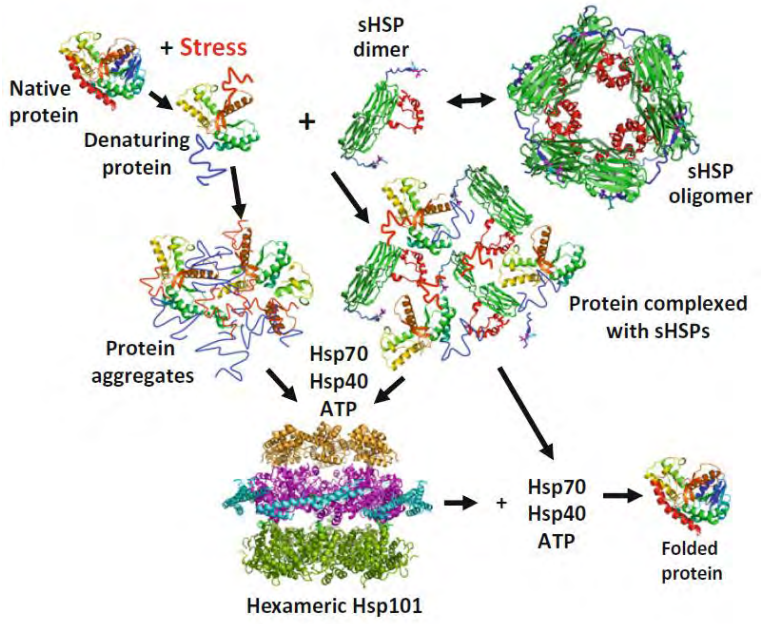

Figure 2 : Proposed model for the mechanism of sHSP chaperone action. As proteins denature due to stress, the sHSP equilibrium shifts from primarily the oligomeric to a dimeric state and dimers contact the denaturing proteins. ATP-dependent HSPs can either contact the aggregated substrates directly or interact with substrates bound to sHSPs to refold the substrates, though the process is more efficient with sHSPs. From Santhanagopalan et al., 2015.

Arabidopsis sHSPs

In *Arabidopsis thaliana*, there are 19 identified sHSP genes (Figure 3). While each of these sHSPs are distinct, they are homologous to sHSPs in other species. This model plant contains six CI proteins: HSP17.4, HSP17.6A, HSP17.6B, HSP17.6C, HSP17.8, and HSP18.1. There are also two class II sHSPs: HSP17.6 and HSP17.7. Additionally, there is one each of class III (HSP17.4), class IV (HSP15.4), class V (HSP21.7), and class VI sHSPs (HSP18.5). These are all known in to be located in the cytosol and lack a targeting peptide as depicted in Figure 3, except for HSP17.4-CIII, which has an internal nuclear targeting sequence. *A. thaliana* has one sHSP that localizes to the endoplasmic reticulum (HSP22.0) and one sHSP that localizes to peroxisomes (HSP15.7). There is one sHSP known to localize only to mitochondria (HSP26.5) and one known to localize only to the chloroplast (HSP25.3). However, there are two proteins,

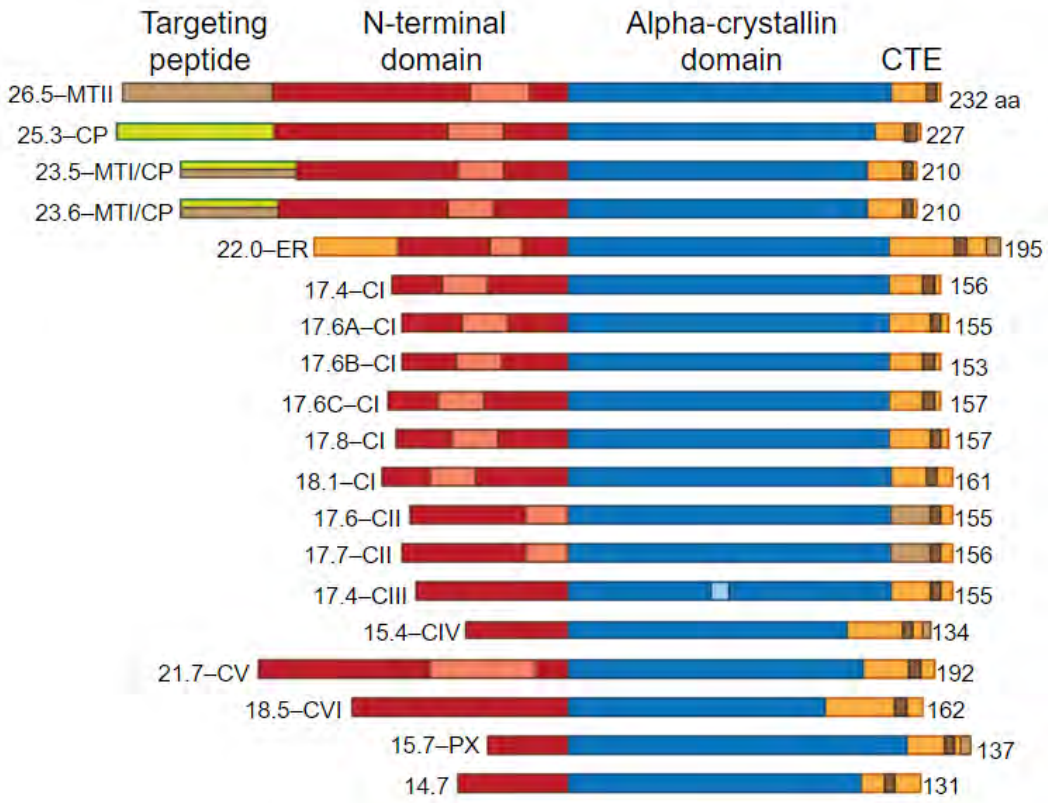

Figure 3: Domain structure of the 19 sHSPs in *Arabidopsis thaliana*. The NTD is illustrated in red, ACD in blue, and CTE in orange. The targeting peptide, if present, is in front of the red NTD. There are 6 classes of sHSPs in *A. thaliana* that are targeted to organelles including chloroplasts (CP), Mitochondria (MTII), endoplasmic reticulum (ER), peroxisomes (PX), nucleus (CIII), and both to the mitochondria and chloroplasts (MTI/CP). There are also 5 classes sHSPs (CI, CII,CIII, CIV, and CV) that localize to the cytosol and lack a targeting peptide. The four organelle-localized sHSPs in this study are 26.5-MTII, 25.3-CP. 23.5 and 23.6-MTI/CP. From Waters and Vierling, 2020.

HSP23.5 and HSP23.6. that are suggested to dual-localize to mitochondria and chloroplasts (Van Aken et al., 2009). There is little research on these latter two specific proteins.

Mitochondrion and Chloroplast sHSPs

The main focus of this project is the sHSPs in *A. thaliana* that localize or dual-localize to the chloroplast and mitochondrion. The most well-studied sHSP of the four proteins is HSP25.3, which localizes to the chloroplast. In fact, HSP25.3, also known as HSP21, can be found in all land plant chloroplasts. Analysis has shown that sHSPs in the chloroplast did not evolve by a gene transfer from an endosymbiont, but by a gene duplication of a nuclear-encoded sHSP (Waters and Vierling, 1999). It is hypothesized that HSP25.3 assists in maintaining homeostasis in the chloroplast. Early studies had indicated the protein helps protect photosystem II

(Heckathorn et al., 1998). Additionally, research of knockout mutants of this sHSP were observed to show an ivory phenotype during chronic heat stress at germination (Zhong et al., 2013). Previous lab member Parth Patel obtained some evidence for acute heat sensitivity of a HSP25.3 null mutant available in the lab. However, much is still not understood about this chloroplast sHSP.

There is little literature regarding HSP26.5 besides its localization to mitochondria. However, an earlier study showed enhanced thermotolerance in overexpression lines of a mitochondrial sHSP homologue from a different plant species (Sanmiya et al., 2004). This study introduced and overexpressed tomato mitochondrial sHSP gene in tobacco and exposed the plant to heat stress conditions. After heat stress, the overexpressed lines showed higher thermotolerance than control Wild-type plants, while reduced expression lines were more heat sensitive compared to Wild-type plants.

The two sHSPs, 23.5 and 23.6, were considered to be localized only to the mitochondria until one paper reported experiments showing dual localization to mitochondria and plastids (Van Aken et al., 2009). A more recent study indicated an early germination phenotype for over expression lines of HSP23.6 (Ma et al., 2019). This study generated overexpression lines of HSP23.5 and HSP23.6 in *A. thaliana*. After 30 hrs, the HSP23.6 overexpression lines showed a higher germination percentage compared to wild-type plants. However, the overexpression HSP23.5 lines has similar germination percentages to Wild-type plants. There are still many questions regarding the chloroplast and mitochondrial sHSPs that have not been addressed. Their specific function and importance are still largely unknown.

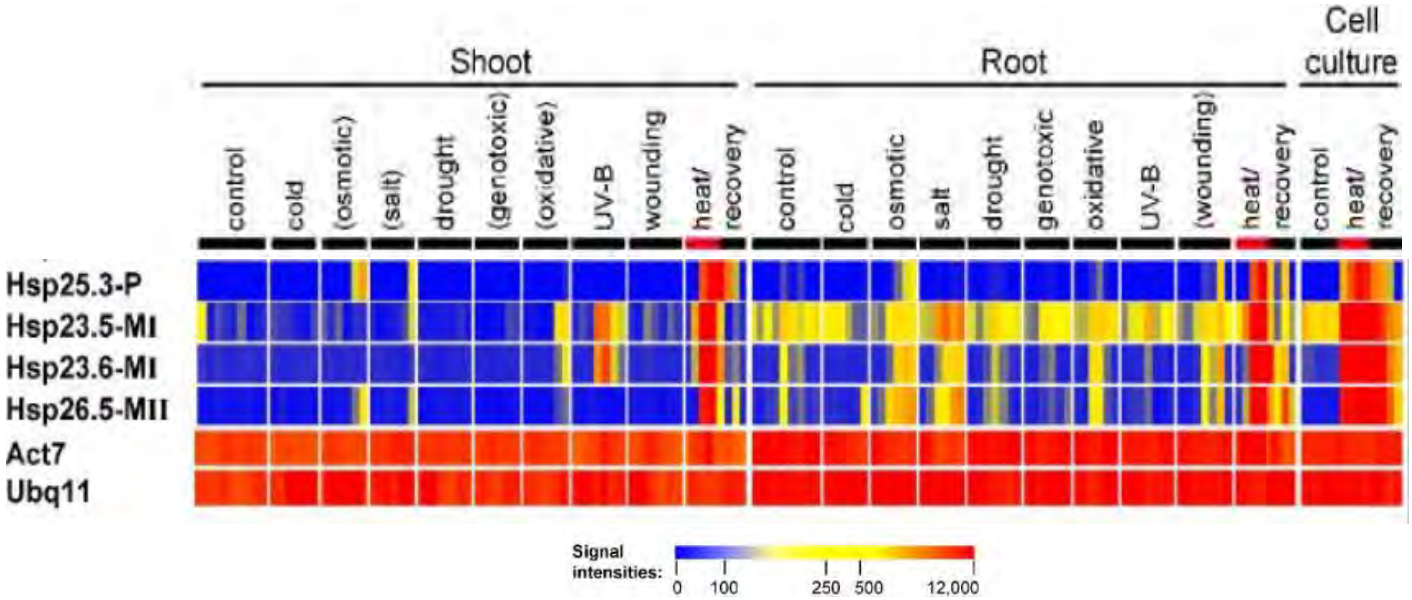

Figure 4: Expression Pattern of organelle-localized sHSPs in response to different stresses. The RNA transcript levels of the four sHSPs were measured through expression profiling under various stresses. Transcript levels in shoots and roots of *A. thaliana* as well as cell cultures (indicated at the top) were determined by microarray analysis. The map is color coded where blue indicates no detected expression through to red indicating high expression (shown in bottom scale). The two genes on the bottom, Act7 and Ubq11, are constitutively expressed and shown as controls. From Siddique et al., 2008.

The expression pattern of the four chloroplast and mitochondrial sHSPs showed the highest expression levels in response to heat stress (Figure 4). The RNA transcript levels were detected from each of the sHSPs of interest in response to various stresses. While some stresses generated an upregulation of the sHSPs, heat stress generated the highest upregulation of expression. Interestingly, HSP23.5 showed low expression at room temperature in shoots, leaves and cell cultures and in response to various stressors in the roots.

Studying the Four Organelle sHSPs

This project focused on the sHSPs that localize to the mitochondrion and chloroplast, the main energy production sites in the cell. The four sHSPs of interest are HSP23.5 (AT5G51440), HSP23.6 (AT4G25200) HSP25.3 (AT4G27670) and HSP26.5 (AT4G27670). HSP25.3, also known as HSP21, localizes to the chloroplast and HSP26.5 localizes only to mitochondria, while HSP23.5 and HSP25.6 have been predicted to dual localize to both organelles. Previous work in the lab also created sHSP-GFP fusion lines to visualize the localization of these sHSPs in order to confirm their targeting to the chloroplast or mitochondrion. Furthermore, the lab has a series of knockout mutants for each of these sHSPs, including triple knock out mutants for sHSPs localized to the chloroplast (*ctko*) and for those localized to the mitochondrion (*mtko*). In addition, there is a quadruple knockout mutant (*qko*) that lacks any of the four organelle sHSPs.

The goal of this project was to develop tools to assess the stress tolerance of mutants of the four organelle-localized sHSPs. One problem is that the HSP25.3 mutant (the chloroplast targeted protein) is a point mutation generated by ethyl methane sulfonate mutagenesis in a different accession background of *A. thaliana* than the other sHSP mutants, which are in the Col background. Although this mutant was backcrossed at least twice to the Col wild type, presence of other point mutations and background alleles could complicate phenotypic analysis and comparison to the other mutants, as well as create problems in the *qko* mutant. To overcome this issue, I worked to create a new mutant of HSP25.3 in the Colombia accession background using CRISPR technology. Having an HSP25.3 mutant in the same background of the other sHSP mutants will be advantageous for phenotypic comparisons, and at the same time will provide a second allele that can be used to validate any observed phenotypes.

A second issue is that the lab has antibodies to detect only three of the four organelle proteins; currently there is no way to detect HSP23.5. This project aims to create an antibody that recognizes HSP23.5, to have a complete set of antibodies against the sHSPs. In addition, this work includes isolating sHSP-GFP transgenic *A. thaliana* lines to confirm the organelle localization of the four proteins. Importantly, this project will work to establish new assay to assess the phenotypes of the sHSP mutant plants. Different stress assays have been conducted on these mutants such as heat stress assays and heavy metal stress assays. However, no distinct phenotype has been observed in the sHSP mutants from current lab research and further study could lead to new insights regarding their functions. Work will include the generation of vectors to use for complementation of the mutant lines to rescue any phenotypes found. Each of these goals is described in more detail below.

This project will assist in providing key understanding of different sHSPs. Every domain of life has sHSPs and they are valuable as the first line of defense in the heat shock response. HSP25.3 is the most well-studied of the four sHSPs under investigation, but still very little is understood about this protein. Even less is known about HSP26.5, HSP23.5, and HSP26.5. The

chloroplast is a major organelle found in plants and it provides energy to the plant through photosynthesis. Additionally, the mitochondrion is another important component in plants that produces ATP for cells. These two organelles are critical in plant energy production and therefore plant survival. It is important to understand how these sHSPs act to protect cellular components and maintain homeostasis in the plant. This project will hopefully lead to the discovery of more information about the sHSPs.

Materials and Methods:

1. *Creating an antibody that recognizes HSP23.5*

Cloning Expression Vector p1416 Encoding the HSP23.5 N-terminus
The Vierling lab has antibodies against the sHSPs targeted to the chloroplast and mitochondrion except for HSP23.5. A construct containing the full-length coding region of the HSP23.5 gene minus the N-terminal 20 amino acid mitochondrial targeting peptide and engineered with an N-terminal Histidine SUMO tag in a pET23b vector (p1405, obtained from Dr. P. Treffon) was used as a source for the gene. Through polymerase chain reaction (PCR) the vector was amplified into the plasmid backbone and an insert, introducing an early stop codon after amino acid 93 in the N-terminus the HSP gene. The following primers were used for the insert:

475 Forward 5' CAGAGAACAGACCGGTGGTTTCAATACCAACGCCGCCAG 3'
476 Reverse 5' GGTGGTGGTGGTGGTGCTCGCTAGATTTCGCTTACCTGGTCC 3'

And the following primers were used to obtain the plasmid backbone:

444 Forward 5'ACCACCGGTCTGTTCTCTGTG 3'
445 Reverse 5' CGAGCACCACCACCACCACCACTG 3'

In a reaction tube, 0.5 µM primer 475 and 0.5 µM primer 476, 1x NEB HF buffer, 200 µM dNTPs each, 0.5 µL Phusion polymerase, 2 µL p1405 (39 ng/µL), and water were added for a total volume of 50 µL. In a second reaction tube, 0.5 µM primer 444, 0.5 µM primer 445, 1x HF buffer, 200 µM dNTPs, Phusion polymerase, 2µL p1405, and water were added for a total volume of 50 µL. The PCR was run at 98°C for 2 mins initially, then for 30 cycles at 98°C for 30 sec, 63°C for 30 sec, and 72°C for 2 mins, then a final 2 mins at 72°C. The PCR fragments were separated on a 1% agarose Tris-acetate-EDTA (TAE) gel at 120V. The two fragments were extracted from the gel using a Thermo Fisher GeneJET Gel Extraction kit. The extracted fragments were added to one PCR tube with 5 µL of Gibson Assembly master mix consisting of three enzymes: T5 exonuclease, Phusion DNA polymerase, and Taq DNA ligase (made and supplied by Dr. Patrick Treffon) for a 10 µL total reaction volume. The reaction was incubated in a thermocycler at 50°C for 4 hrs. The Gibson assembly cloning products were transformed into DH5α *E. coli* cells. The DH5α *E. coli* cells were thawed on ice from -80°C. Once thawed, 5 µL of the Gibson assembly cloning product (p1416) was added to competent *E. coli* cells. The tube was then placed in ice for 30 mins. The competent cells were submerged 2/3 of the way into at 42°C water bath for 45 sec. The cells were immediately placed on ice for 3 mins proceeding the heat shock. After 3 mins, 250 µL of lysogeny broth (LB) media was added to the competent cell tube. The cells were then placed in the incubator at 37°C and 200 RPM. After 45 mins, 50 µL of the culture was spread onto an LB agar plate with 100 µg/mL ampicillin. The plate was placed in

a 37°C incubator for 16 hrs. A pipette tip was used to resuspend each plate colony in 30 µL of sterile water. A colony PCR was performed using the resuspended colonies as templates with the insert primers listed above (475 and 476). The thermocycler conditions were at 98°C for 8 mins initially, then for 30 cycles at 98°C for 30 sec, 63°C for 30 sec, and 72°C for 2 mins, then a final 2 mins at 72°C. A 1% agarose TAE gel was run at 120V to visualize bands, indicating positive colonies for p1416. An overnight culture of the remaining positive colony was made in 5 mL of LB media with antibiotics (100 µg/mL ampicillin) and grown at 37°C and 200 RPM for 16 hrs. The plasmid DNA was isolated using a GeneJET miniprep kit. The plasmid DNA was confirmed by sequence analysis and the new plasmid was designated as p1416.

Expression of the HSP23.5 N-terminus from plasmid p1416
The isolated DNA of p1416 was transformed into LOBSTR (low background strain; supplied by Dr. Patrick Treffon) *E. coli* using the same transformation protocol as above. The transformed cells were inoculated into 50 mL of LB media with 100 µg/mL ampicillin and 20 µg/mL chloramphenicol and grown for 16 hrs at 37°C and 200 RPM. The 50 mL was then inoculated into 950 mL of LB media with half the concentration of antibiotics previously used and grown at 37°C and 200 RPM until an OD_{600} of 0.416 was achieved. Protein expression was then induced by adding IPTG to a final concentration of 0.5 mM and cells grown for an additional 16 hrs at 22°C and 200 RPM. Samples of 1.0 mL were taken right before and after induction and labeled T0 and T24, respectively. The OD readings of the ΔC-HSP23.5 protein at T0 and T24 were 0.418 and 2.828, respectively. The 1 mL T0 sample and 150 µL of the T24 sample was pelleted for 5 min at 13000 RPM. The pellets were resuspended in 10 µL H_2O and 90 µL of SDS sample buffer. SDS-PAGE analysis was performed on the samples as described below for the chromatography fractions. The T0 sample was loaded twice with two different volumes first with 30 µL and then with 40 µL. The T24 samples were all loaded at 5 µL.

Cleavage and Purification of the HSP23.5 N-terminus (ΔC-Hsp23.5)
The induced culture of p1416 was pelleted at 5000 RPM for 15 mins at 4°C. The pellet was resuspended in 20 mL lysis buffer (50 mM NaH_2PO_4, 300 mM NaCl, and 10 mM imidazole) with a Thermo Fisher protease inhibitor tablet. The cells were disrupted through a microfluidizer in the lysis buffer. The fluidized solution was spun down at 20000 RPM at 4°C for 45 mins. The supernatant was transferred to a new sterile centrifuge tube and small samples taken of both the pellet and supernatant. The supernatant had dithiothreitol (DTT) added for a final concentration of 1.0 mM. The remaining supernatant was separated with an ÄTKA Start fast protein liquid chromatography (FPLC) instrument using a Cytiva HisTrap HP 1 ml column at 4°C. The column was primed and equilibrated with 10 column volumes (CV) of lysis buffer. The supernatant loaded around 35 mL on the column, washed with 15 CV lysis buffer, and eluted with 5 CV of elution buffer from the column. The flow rate was 1 mL per min and the elution from the column was collected in 1 mL fractions. Samples of 30 µL were taken of the flow-through and wash, and 10 µL samples were taken of the elution fraction. The remaining elution fraction (around 5 mL) was transferred to a dialysis tube. To the dialysis tube, 10 µL ULP1 SUMO protease (supplied by Patrick Treffon) and a final concentration of 2 mM DTT was added. The dialysis tube was clamped and submerged in 1X PBS on a stirrer overnight at 4°C. A 10 µL sample of the cleaved elution fraction was collected. The remainder of the elution fraction was about 4.5 mL. Previous purification attempts resulted in the cleaved ΔC-Hsp23.5 protein remaining bound to the column and an ion exchange chromatography was run instead. The FPLC instrument was

used with a Cytiva HiTrap Q FF 5 mL anion column. The cleaved elution sample in 1 X PBS was mixed at a 1:1 ratio with 20 mM TrisH7.5. The now 8.5 mL fraction was mixed and incubated for 10 mins at 4°C prior to the ion exchange chromatography. The column was equilibrated with 5 CV of 1X PBS. The 8.5 mL sample was now set to flow through the anion column and washed with 5 CV of 20 mM Tris pH 7.5 buffer at a flow rate of 5 mL/min. The column was washed with 20 mM Tris pH 7.5 buffer mixing with a gradually increasing amount of 20 mM Tris 1 M NaCl buffer in a gradient elution until 100% of 20 mM Tris 1 M NaCl buffer was being used over 20 CV. Fractions were collected in 5 CV. There were samples from 9 of the 5 CV fractions that were collected in 30 µL samples.

SDS PAGE of Chromatography Fractions

The samples collected of the pellet, supernatant, flow-through (30 µL), wash (30 µL), elution (10 µL), and elution after dialysis (10 µL) were prepared with sterile MQ-H_2O and 5X SDS sample buffer to a final concentration of 1x SDS sample buffer (40 mM Tris-HCl, 12.5% glycerol, 0.625 g sodium dodecyl sulfate, 0.01 g bromophenol blue, 20 mM dithiothreitol) and heated for 10 mins at 95°C. The samples collected from the ion exchange chromatography (30 µL each), were prepared with sterile MQ-H_2O and a final concentration of 1X SDS sample buffer and then heated for 10 mins at 95°C. The fractions were loaded onto 18% SDS polyacrylamide gel and run at constant 40 mA. The fractions that contained the expected molecular weight bands of ΔC-Hsp23.5 (6.6 kDa) were centrifuged together through a 3000 Da cut-off filter at 5000 RPM and 4°C until 2 mL total volume was achieved.

Protein Concentration Determination

A Bicinchoninic acid (BCA) assay was performed to measure the concentration of the purified protein. The standards Lysozyme and Bovine serum albumin (BSA) were each made in 0, 0.25, 0.125, 0.25, 0.50, 0.75, 1.0, 1.5, and 2.0 mg/mL concentrations in 20 mM Tris pH 7.5 buffer. In a 96-well plate, 5 µL of each concentration of each protein standard was loaded in triplicate. The 5 µL of the 2 mL concentrated ΔC-Hsp23.5 protein was loaded onto the plate in triplicate. A BCA working reagent was made with 50 parts of Thermo Fisher Reagent A and 1-part Thermo Fisher BCA Reagent B. To each well with protein, 200 µL of BCA working reagent was added. The wells were mixed through pipetting and the plate incubated at 37°C for 30 min. The plate was allowed to cool to room temperate (RT) for 5 mins and then the absorbance was measured at 562 nm on a plate reader. A standard curve was created using the average of the triplicate standard values versus the known concentration. The average absorbance level of ΔC-Hsp23.5 was used to solve for concentrations for both standard curves. An SDS-PAGE analysis was also used to measure ΔC-Hsp23.5 protein concentration. An 18% SDS gel was run under the same conditions described above with different volumes (1, 3, 5, 10, 15, and 20 µL) of a 1:10 diluted ΔC-Hsp23.5 sample and known amounts of lysozyme standard (0.2, 0.4, 0.6, 0.8, and 1.0 µg). Image J analysis was used to calculate the area of the bands on the gel and a standard curve was calculated for the lysozyme standard. The diluted ΔC-Hsp23.5 concentration was calculated using the standard curve.

2. *CRISPR/cas9* HSP25.3 Mutant

CRISPR/cas9 Cloning

To create a null mutant for HSP25.3 in the *A. thaliana* Colombia background, the following protocol was obtained from A CRISPR/Cas9 toolkit (Xing et al., 2014). Two target sequences were identified (by Prem Patel) in the HSP25.3 gene using CRISPR-P v2 software. These target sequences would create a 488 bp deletion of the HSP25.3 gene in the middle of two exons flanking the single intron in the gene. The following primers were designed to insert the target sequences into the construct plasmid named p1385 (also known as pCBC-DT1T2) which is plasmid containing the gRNA scaffolding gene that can be engineered to contain two target guide RNAs.

DT1-BsF 5'ATATATGGTCTCGATTGCGAAACCGAGAACGGTGTAGGTT 3'
DT1-F0 5'TGCGAAACCGAGAACGGTGTAGGTTTTAGAGCTAGAAATAGC 3'
DT2-R0 5'AACCTTTGATGTCCCACGGTGCACAATCTCTTAGTCGACTCTAC 3'
DT2-BsR 5'ATTATTGGTCTCGAAAC CTTTGATGTCCCACGGTGCACAA 3'

In a reaction tube, 20 µM primers DT1-BSF and DT2-BsR and 1 µM of primers DT1-F0 and DT2-R0 were added. In addition, 5x HF buffer, 200 µM dNTPs, Phusion polymerase, p1385, and water were added for a total volume of 50 µL. The reaction was placed in a PCR thermocycler at 98°C for 2 mins and 98°C for 15 sec, 63°C for 30 sec, and 72°C for 1 min at 30 cycles, then 72°C for 5 mins. To the sample, 10 µL of 5X DNA loading dye was added and the 60 µL sample was separated on a 1% agarose TAE gel. The bands were extracted using Thermo Fisher GeneJET Gel Extraction kit. A Golden Gate cloning reaction was then performed with the purified fragments to clone the p1385 gRNA products into the destination vector known as plasmid p1384, which contains the Cas9 gene controlled by an egg specific promoter, EC1.2 (Wang et al., 2015). To a reaction tube, 200 ng of the PCR product, 200 ng of p1384 (also known as pHSE401), 10X T4 DNA ligase buffer, 10X BSA, BSAI (NEB), High Concentrated T4 DNA ligase, and sterile H_2O for a total volume of 15 µL. The reaction was run in a thermocycler at 37°C for 5 hrs, 50°C for 5 mins, and 80°C for 10 mins. The sample was then transformed into Thermo Fisher TOP10 competent cells following the same transformation protocol and confirmed with colony PCR and sequencing using the following primers:

357 5'TGTCCCAGGATTAGAATGATTAGGC 3'
358 5' AGCCCTCTTCTTTCGATCCATCAAC 3'

The sequencing results from Macrogen were used in a sequence alignment using Benchling software.

Agrobacterium Transformation

The confirmed clones containing the CRISPR guide sequences were inoculated for overnight cultures following the same protocol as above except using 100 µg/mL kanamycin. Three mL of the overnight culture was used to purify DNA using a Thermo Fisher GeneJET Mini-Prep kit. The new transformed vector containing the Cas9 gene and target gRNAs was renamed p1417. Agrobacterium competent cells (made and provided by the Vierling Lab) were thawed from -80°C and 0.5 µL of p1417 plasmid DNA was added and mixed with a pipette. The cells containing the plasmid were transferred to a cuvette with a lid, placed into an electroporator and shocked with 1800V for 5 millisecs. Immediately after, 1 mL of LB liquid media was added to the cuvette and pipetted up and down. The contents were transferred to a clean microcentrifuge

tube and incubated at 28°C and 200 RPM for 3 hrs. After 3 hrs, 20 µL from the incubated cells was spread over an LB agar plate containing 100 µL/mL kanamycin and 50 µL/mL gentamicin (antibiotic resistance gene in the Agrobacterium). The plate was incubated at 28°C for several days. After two days, colonies were cultured overnight in 5 mL LB media with both antibiotics at 28°C and 200 RPM. The cultures were used for floral dip transformation.

Floral Dip Transformation

The CRISPR/cas9 HSP25.3 plasmid (p1417) was transformed into *A. thaliana* plants. *A. thaliana* wild-type plants were grown with 9 plants per a pot until they were flowering. The 5 mL overnight culture of p1417 was inoculated into a larger 300 mL culture of LB with required antibiotics and allowed to grow overnight with the same parameters. The 300 mL culture was pelleted and resuspended to an OD_{600} of around 0.8 in a 5% sucrose solution. Silwet L-77 was added to 0.0166% v/v and the solution was thoroughly mixed. The wild-type plants were carefully dipped into the agrobacterium solution, completely submerging the plant until the rosette, for at least one min. The plants were then covered to create high humidity for 24 hrs. The dipped plants were watered and allowed to grow normally in a growth chamber. As the plants became mature, they were allowed to dry, and the seeds were harvested.

3. *HSP-GFP Localization*

HSP-GFP Construct Screening

The four sHSPs of interest are predicted to localize to organelles and the Vierling Lab has tagged the sHSPs with GFP to confirm localization. Vectors containing HSP23.5, HSP23.6, HSP25.3, and HSP26.5 genes from the native promoter until before the stop codon translationally fused to the GFP gene were created by previous lab member, Parth Partel, who also transformed them into Agrobacterium and introduced them by floral dipping into *A. thaliana* Wildtype and Quadruple Knockout (*qko*) mutants of the four sHSP genes. These *qko* mutants were also generated by Parth Patel, by crossing and genotyping the four sHSP mutant plants (See Figure 9A). Parth Patel also selected the first generation (T1) plants on 0.5x Murashige and Skoog (MS) media with 0.5% sucrose, 0.8% agar, and 15 µg/mL hygromycin for survival. The T1 plants were grown until matured, and seeds harvested. The T2 seeds from these plants were plated on the same MS media with hygromycin by former lab member Tianxiang Liu and screened for lines showing 3:1 segregation of the introduced resistance marker. I took over at the point of selecting three seedlings from each identified 3:1 segregating line from each background and transferring them to soil. The seeds from the T2 generation, known as T3 seeds, were harvested, and screened for no segregation on MS media with hygromycin to identify homozygous lines for each HSP-GFP fusion construct in both backgrounds. These plants were transferred to soil, allowed to grow, and then were harvested for the seeds.

Confocal Microscopy of sHSP-GFP in A. thaliana

Three of the sHSPs of interest are predicted to localize to the mitochondrion (HSP26.5, HSP23.5, and HSP23.6), and therefore the mitochondrion was the focus for the localization of these sHSPs. Three seeds of each HSP26.5, HSP23.5, and HSP23.6-GFP fusions were placed on two plates of 0.5x MS 0.5% sucrose, 0.8% agar media. Three seeds of Mito-GFP, mitochondria tagged with GFP, were placed on each plate as controls (Supplied by Dr. David Logan; Logan

and Leaver, 2000). The plates were stratified in the dark at 4°C for 2 days. The seeds were then moved to a 22°C incubator with a day/night light cycle and allowed to grow for 5-9 days until the roots were long enough to view in a microscope. Once grown, one plate was placed in a 38°C incubator in the dark for 60 mins, while the other plate remained at room temperature. The heated plate was moved back to room temperature for at least 60 mins to allow sHSPs to accumulate. The seedlings from both plates were then incubated in liquid 0.5x MS media with 500 nM Thermo Fisher MitoTracker Orange for 10 mins. Seedlings were transferred to regular liquid 0.5x MS media. The roots of the seedlings were visualized with an Olympus FV10-ASW Laser Confocal Microscope at 60x magnification. The GFP was visualized using an excitation wavelength of 488 nm and emission wavelength between 490 and 540 nm. The red fluorescence from the MitoTracker was visualized with an excitation wavelength of 559 and emission wavelength between 575 and 675 nm. Three of the sHSPs of interest are also predicted to localize to the chloroplast (HSP25.3, HSP23.5, HSP23.6). Three seeds of each genotype were placed on two separate plates of 0.5x MS 0.5% sucrose, 0.8% agar media. Three Col seeds were also plated on each plate as controls. The cotyledons were visualized with the same microscope and the wavelengths as used for the mitochondria at 60x magnification. The seeds were stratified in the dark at 4°C for 2 days. The seeds were then moved to a 22°C incubator with a day/night light cycle and allowed to grow for 5-9 days until the cotyledons were large enough to visualize in the microscope. The plates were heat treated under the same conditions as mentioned above.

4. *Generating Complementation vectors for the sHSP mutants*

Genomic DNA Extraction

To generate complementation vectors for the four sHSPs, the individual genes needed to be amplified from genomic DNA to obtain the 3' non-coding and other downstream sequences. Four wild-type, two-week old seedlings were extracted from soil and placed into a mini-centrifugation tube. The plant tissues were ground with a pestle for 30 sec. Then 400 µL of Edwards Buffer (200mM Tris, 25 mM EDTA, 250 mM NaCl, 0.5% SDS, pH 8) was added to the tube. The same pestle was used to grind the tissue again for 10-15 sec. The tube was then vortexed for 5 sec and centrifuged at room temperature and 13,000 rpm. The supernatant was transferred to a fresh microfuge tube and 300 µL was added. The new tube was inverted several times and then allowed to sit for two mins at room temperature. The microfuge tube was centrifuged again for 10 mins. The supernatant was discarded, and the pellet was washed with 700 µL 70% EtOH. The sample was centrifuged again for 5 mins and the supernatant discarded. The pellet was allowed to air dry at 38°C and then resuspended in 40 µL sterile H_2O.

Complementation Vector for HSP23.5

The HSP23.5-GFP plasmid created by Parth Patel (PP5) was used as the source of the HSP23.5 native promoter and coding sequence. PP5 lacks the HSP23.5 stop codon and is instead fused to GPF at the C-terminus and contains a kanamycin-resistant and hygromycin-resistant gene. The goal was to remove the GFP gene from the vector and add in the stop codon, 3' UTR, and native terminator of HSP23.5. This would create a complementation vector for HSP23.5 (p1425). For Gibson Assembly cloning the construct was broken into three fragments: A, B, and C. Fragments A and B were amplified from the plasmid backbone and Fragment C was the stop codon, 3'UTR, and native terminator amplified from genomic DNA. The following primers were used to amplify fragment A from PP5.

495: 5’ CCAAAATAAAACACTCTAGTCAACGTTTATGTGACGAATATTG 3’
IsoKan1: 5’ GCCTGTTCCAAAGGTCCTGCACTTTG 3’

The following primers were used to amplify Fragment B from PP5

496: 5’ GTTCGTGTCGGCATCGTCAGATCGGGAATTCG 3’
IsoKan2: 5’ CAAAGTGCAGGACCTTTGGAACAGGC 3’

The following primers were used to amplify Fragment C from genomic DNA

497: 5’ CAATATTCGTCACATAAACGTTGACTAGAGTGTTTTATTTTGG 3’
498: 5’ CGAATTCCCGATCTGACGATGCCGACACGAACGAGT 3’

The PCR reactions were completed in 50 µL reactions (1X Phusion NEB HF Buffer, 0.5µM forward primer, 0.5 µM reverse primer, 200 µM dNTP, 0.5 µL homemade Phusion polymerase, and sterilized H_2O) in a thermocycler set to 98°C for 2 mins initially, then for 30 cycles at 98°C for 30 sec, 55°C for 30 sec, and 72°C for 6 mins, then a final 10 mins at 72°C.
Each of the PCR reactions were run on a 1% agarose TAE gel and underwent gel extraction with the GeneJET Gel Extraction kit. Fragment A had a concentration of 20.9 ng/µL, Fragment B had a concentration of 32.3 ng/µL and Fragment C had a concentration of 156 ng/µL. In a PCR reaction tube, 4.8 µL Fragment A, 3.2µL Fragment B, 0.2 µL Fragment C, 1.8 µL H_2O, and 10 µL homemade Gibson Assembly mix was added. The reaction tube was placed into a thermocycler at 50°C for 4 hrs. The Gibson Assembly product created the complementation vector construct named p1425. Using competent cells, 5 µL of the Gibson Assembly product was transformed into Thermo Fisher DH5α *E. coli* cells. Colonies were made into overnight cultures with 5 mL LB media and 100 µg/µL kanamycin. The cells were isolated for DNA using a Thermo Fisher Plasmid-mini prep kit. A restriction digest was completed to confirm the complementation vector. In a reaction tube, 1 µL of restriction enzyme NEB EcoRV-HF, 1x NEB rCutsmart buffer, 1 µg p1425 DNA, and H_2O to make a 50 µL reaction were added. The reaction tube was then incubated at 38°C for 1 hr and then run on a 1% agarose TAE gel. The restriction enzyme had three cut sites on the p1425 construct to generate three DNA bands at 1300 bp, 2600 bp, and 7000 bp. DNA from PP5 was also used in a restriction digest as a control with the same expected cut sites. Four clones were confirmed with the restriction digest by showing these three bands on a gel.

Complementation vector for HSP23.6
The starting plasmid for the HSP23.6 complementation vector (p1426) was an HSP23.6-GFP plasmid (PP6) created by Parth Patel, and the same procedures followed as described above. Fragments A and B were amplified from the plasmid backbone and Fragment C was the stop codon, 3’UTR, and native terminator amplified from genomic DNA. The following primers were used to amplify fragment A from PP6.

518: 5’ CGTCGACGTTTTTAGTTGATCTCGATCTG 3’
IsoKan1: 5’ GCCTGTTCCAAAGGTCCTGCACTTTG 3’

The following primers were used to amplify fragment B from PP6.

519: 5’ GTCGACGGACTGGTCTAGATCGGGAATTCGTAATC 3’
IsoKan2: 5’ CAAAGTGCAGGACCTTTGGAACAGGC 3’

The following primers were used to amplify fragment C without the Gibson Assembly overhangs from genomic DNA.

565: 5’ TAAaaacgtcgacgttttttttc 3’
566: 5’ agaccagtccgtcgacaactt 3’

Each of these reactions were completed in 50 µL samples (NEB Q5 Polymerase, 1X NEB Q5 Reaction Buffer, 0.5µM forward primer, 0.5 µL reverse primer, 200 µM dNTP, and sterile H_2O). The fragments were then run on 1% agarose TAE gel and gel extracted with a Thermo Fisher GeneJet Gel Extraction kit.

The Gibson Assembly overhangs were added to Fragment C with the following primers using the same PCR reaction and reagents listed above with 30 ng of Fragment C DNA (without the Gibson Assembly overhang):

517: 5’ CAGATCGAGATCAACTAAAAACGTCGACG 3’
520: 5’ GATTACGAATTCCCGATCTAGACCAGTCCGTCGAC 3’

A concentration of 54.8 ng/µL was obtained for Fragment A, 21.5 ng/µL for Fragment B, and 35.2 ng/ µL for Fragment C with the Gibson Assembly overhangs added. The three fragments were added to a reaction tube and a Gibson Assembly reaction was followed as described above with 1.8 µL Fragment A, 4.5 µL Fragment B, 0.4 µL Fragment C, 3.3 µL H_2O and 10 µL homemade Gibson Assembly Mix. The Gibson Assembly product generated the HSP23.6 complementation vector (p1426). Five µL of the Gibson Assembly product was used for a transformation into Thermo Fisher DH5α *E. coli* cells. Colonies were selected on LB agar plates with proper antibiotics and made into overnight cultures and purified for DNA using Thermo Fisher Mini-prep plasmid kit. Two positive colonies were confirmed through colony PCR using primers 517 and 520 (listed above).

Complementation vector for HSP25.3
The starting plasmid for the HSP25.3 complementation fragment was an HSP25.3-GFP construct (PP7) generated by previous Lab member Parth Patel. The same protocol was followed as listed above to generate a complementation vector for HSP25.3 (p1427). The following primers were used to amplify Fragment A from PP7:

522: 5’ GTTGATCGAGTCCTACTGAATCTGGACATC 3’
IsoKan1: 5’ GCCTGTTCCAAAGGTCCTGCACTTTG 3’

The following primers were used to amplify Fragment B from PP7:

523: 5’ CGTTCATAAGATATGAGATCGGGAATTCG

IsoKan2: 5’ CAAAGTGCAGGACCTTTGGAACAGGC 3’

The following primers were used to amplify Fragment C without Gibson Assembly overhangs from WT genomic DNA:

567: 5’ TAGgactcgatcaacattatcctc 3’
568: 5’ catatcttatgaacgattcc 3’

The PCR products were run on an agarose gel and extracted for DNA as described above. Fragment A yielded a DNA concentration of 36.7 ng/ µL and Fragment B yielded a DNA concentration of 49.6 ng/ µL. The overhangs were added onto Fragment C using 30 ng of DNA in the same PCR reaction described above. The following primers were used:

521: 5’ GATGTCCAGATTCAGTAGGACTCGATCAAC 3’
524: 5’ GCCTGTTCCAAAGGTCCTGCACTTTG 3’

Fragment C with the Gibson Assembly overhangs were run on an agarose gel and extracted for DNA to report a concentration of 29 ng/ µL. The three fragments were used in a Gibson Assembly reaction using 2.7 µL Fragment A, 2.1 µL Fragment B, 0.8 µL Fragment C, and 4.4 µL H_2O. The Gibson Assembly product generated the HSP25.3 complementation vector (p1427). The Gibson assembly product was transformed into *E. coli* and grown on LB plates with antibiotics. Overnight cultures were made of colonies present on the plates and DNA was isolated. Colony PCR was performed to confirm 3 positive colonies following the same guidelines mentioned previously using primers 521 and 524.

Complementation vector for HSP26.5
The starting plasmid for the HSP26.5 complementation vector was the HSP26.5-GFP line (PP8) generated by former lab member Parth Patel. The cloning of the construct was completed under the same guidelines as the other complementation vectors above. Fragment A was amplified from PP8 with the following Primers:

526: 5’ CACCGTATCTCTTCTACTCAACAGAAATCTCCTG 3’
IsoKan1: 5’ GCCTGTTCCAAAGGTCCTGCACTTTG 3’

Fragment B was amplified from PP8 with the following primers:

527: 5’ CTTTTAGTTTGGTATTAGATCGGGAATTCGTAATC 3’
IsoKan2: 5’ CAAAGTGCAGGACCTTTGGAACAGGC 3’

Fragment C was amplified without the Gibson Assembly overhangs from WT genomic DNA using the following primers:

569: 5’ TAGaagagatacggtgtcgtttttg 3’
570: 5’aataccaaactaaaagaagg 3’

The Gibson Assembly overhangs were added to Fragment C following the same PCR protocol listed previously using 30 ng of Fragment C DNA and the following primers:

525: 5’ CAGGAGATTTCTGTTGAGTAGAAGAGATACGGTG 3’
528: 5’ GATTACGAATTCCCGATCTAATACCAAACTAAAAG 3’

The PCR reactions were run on an agarose TAE gel and extracted for DNA. Fragment A had a concentration of 12.3 ng/µL. Fragment B had a concentration of 29.3 ng/µL. Fragment C with the Gibson Assembly overhangs had a concentration of 52.2 ng/µL. The Gibson Assembly cloning was done following the same procedure as above but with 7.3 µL Fragment A DNA, 2.4 µL Fragment B DNA, and 0.3 µL fragment C DNA. The Gibson Assembly products generated the HSP26.5 complementation vector (p1428). The products from the Gibson Assembly were transformed in Thermo Fisher DH5α *E.coli* cells and grown on LB agar plates with antibiotics. Colonies were made into overnight cultures and isolated for DNA using a Thermo Fisher mini-prep kit. A restriction digest was done under the same conditions as listed above (Under HSP23.5 complementation vector) but using 1 µg of p1428 DNA and 1 µL NEB XbaI restriction enzyme. This restriction digest made three cuts at 600 bp, 3000 bp, and 10000 bp on positive plasmids. PP8 was also used as a control for the restriction digest and expected the same cut sites. One positive clone was confirmed through the restriction digest which yielded the same expected band sizes on a 1% agarose TAE gel.

5. *Heat Stress Assays on sHSP mutants*

Seed Setting Heat Stress Assay
Heat stress may have an effect on seed setting in *A. thaliana,* therefore, experiments were performed to find the optimal temperature that affects seed setting in plants to generate a heat stress protocol. Eight plants each of Col wild type and the heat-sensitive HSP101 (AT1G74310) null mutant *hot1-3* were grown in 7cm x 7cm square single pots with soil at 22°C and 16-hr day with 57 µL light intensity and 8-hr night cycles until at least five siliques had matured on all of the plants (Hong and Vierling, 2001). Then, a flower in stage 12-13 development was marked with red thread (Figure 19). Three plants of each genotype were heat stressed in a dark incubator at 34°C or 38°C for 6 hrs over two days. Two plants of each genotype were kept at room temperature in the dark during the heat stress as controls. The heat stress was completed at 4 hrs into the light cycle over the two-day period. After heat stressing, the plants were returned to normal growth conditions for 10-12 days until the plants were fully mature. The siliques on each plant were then numbered and their length measured. The silique measurements for each genotype at each heat treatment were averaged together and graphed for data analysis.

Results:

Generating an antibody that recognizes HSP23.5

The goal of this part of my project was to clone, express, and purify a protein to use for production of an antibody to recognize HSP23.5. The two sHSPs expected to dual-localize to the mitochondria and chloroplasts (HSP23.5 and HSP23.6) are similar proteins, having an amino

A)

```
HSP23.5         1 MASSSALALRRLLSSSTVAVPRALRAVRPVAASSRLFNTNAARNYE----     46
                  .:|||||:||||||  ..||:...:|| |.|||||||||.|:|:
HSP23.6         1 --MASALALKRLLSSS--IAPRSRSVLRP-AVSSRLFNTNAVRSYDDDGE     45

HSP23.5        47 --DGVDRNHHSNRHVSRHGGDFFSHILDPFTPTRSLSQMLNFMDQVSEIP     94
                    ||||.   ..|.|.|..|||||.:.|||:||||:||:||.|||..|.|
HSP23.6        46 NGDGVDL---YRRSVPRRRGDFFSDVFDPFSPTRSVSQVLNLMDQFMENP     92

HSP23.5        95 LVSATRGMGASGVRRGWNVKEKDDALHLRIDMPGLSREDVKLALEQNTLV    144
                  |:||||||||||.||||::|||||||:||||||||||||||||||:|||
HSP23.6        93 LLSATRGMGASGARRGWDIKEKDDALYLRIDMPGLSREDVKLALEQDTLV    142

HSP23.5       145 IRGEGETEE--GEDVSGDGRRFTSRIELPEKVYKTDEIKAEMKNGVLKVV    192
                  |||||:.||  ||:.....|||||||.||:|:||.|||||||||||||||
HSP23.6       143 IRGEGKNEEDGGEEGESGNRRFTSRIGLPDKIYKIDEIKAEMKNGVLKVV    192

HSP23.5       193 IPKIKEDERNNIRHINVD    210
                  |||:||.|||::|.|.::
HSP23.6       193 IPKMKEQERNDVRQIEIN    210
```

B)

```
# Gap penalty: 10.0
# Extend penalty: 0.5
# Length: 218
# Identity:     145/218 (66.5%)
# Similarity:   169/218 (77.5%)
# Gaps:          16/218 ( 7.3%)
# Score: 690.5

HSP23.6         32 FNTNAVRSYDDDGENGDGVDLYRRSVPRRRGDFFSDVFDPFSPTRSVSQV      81
                   |||||.|:|:|..:.....:    |.|.|..|||||.:.|||:||||:||:
p1416            1 FNTNAARNYEDGVDRNHHSN---RHVSRHGGDFFSHILDPFTPTRSLSQM      47

HSP23.6         82 LNLMDQFME      90
                   ||.|||..|
P1416           48 LNFMDQVSE      56

# Gap penalty: 14
# Extend penalty: 4
# Length: 59
# Identity:      31/59 (52.5%)
# Similarity:    39/59 (66.1%)
# Gaps:           3/59 ( 5.1%)
# Score: 141
```

Figure 5: Protein Alignment of HSP23.5, HSP23.6, and ΔC-Hsp23.5. A) Protein Sequence Alignment of HSP23.5 and HSP23.6. The highlighted yellow portion of HSP23.5 represents the amino acid sequence included in ΔC-Hsp23.5. The vertical lines represent matching amino acids, one dot represents weakly similar properties, and two dots represent strongly similar properties. No dot represents no relationship. B) The protein sequence alignment of HSP23.6 and ΔC-Hsp23.5. Alignments were executed using Pairwise Sequence Alignment software. The Emboss Matcher program was used under Pair format.

acid identity of 66.5% and similarity of 77.5% (Figure 5A). The aim was to express and purify a portion of Hsp23.5 with the least similarity to Hsp23.6 as an approach to produce antisera that would show a strong degree of specificity for reaction with Hsp23.5 vs. Hsp23.6.

The region chosen comprised amino acids 36 to 93 (Fig. 4B), which contain the predicted amino terminus of the mature protein (after cleavage of the mitochondrial targeting sequence). This region is within the sHSP NTD and shows 52.5 % identity and 66.1% similarity between the two proteins. To create the *E. coli* expression plasmid for this fragment (ΔC-HSP23.5) required introducing a stop codon at amino acid 93 starting with the plasmid pET23b-His-Sumo-HSP23.5 (Hsp23.5 in plasmid p1405, obtained from Dr. P. Treffon) that had been designed to express the full length, mature protein. A Gibson assembly cloning reaction was performed to create His-SUMO-ΔC-HSP23.5 (p1416), a 6x His-SUMO tagged truncated HSP23.5 with an early stop codon in the N-terminus replacing amino acid 94. The plasmid was transformed into *E.coli* and confirmed through colony PCR and sequencing. ΔC-HSP23.5 was expressed in LB media and induced with 0.5 mM IPTG (Figure 6). The ΔC-HSP23.5 sample was compared to expression of the full- length HSP23.5 gene from p1416. The expected protein size for His-SUMO-ΔC-HSP23.5 is 18.95 kDa, while the expected band sized for His-SUMO-HSP23.5 is 32.1 kDa. The His-SUMO-HSP23.5 protein was strongly induced by IPTG as evidenced by the major band at the expected size. In contrast, although expression of the His-SUMO-ΔC-HSP23.5 was evident at 18.95 kDa in both the T0 and T24 samples, there was no obvious increase in expression of the protein with the IPTG induction.

Although strong induction of His-SUMO-ΔC-HSP23.5 was not observed, I proceeded with purification of the protein from the induced culture by Fast Protein Liquid Chromatography (FPLC) with a nickel affinity column. Fractions were collected and analyzed by SDS-PAGE

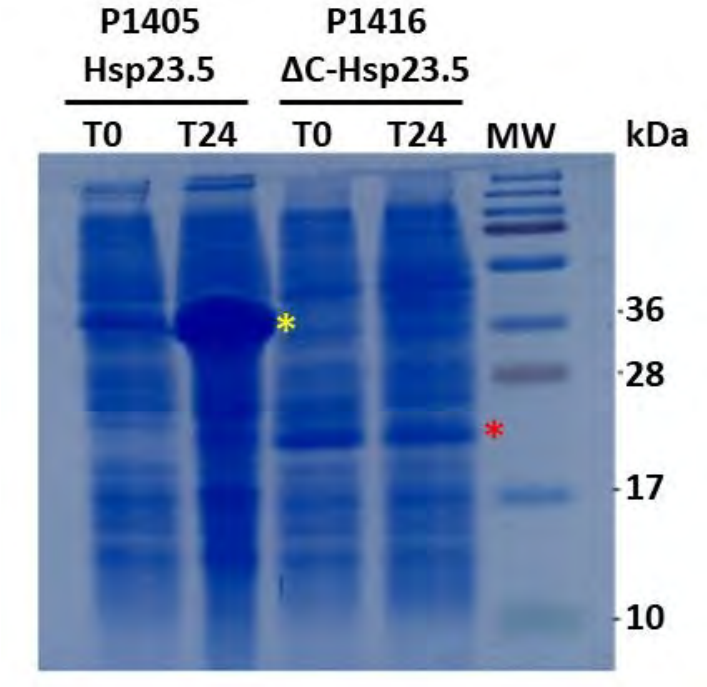

Figure 6: 18% SDS gel of the expression and induction of HSP23.5 (p1405) and ΔC-Hsp23.5 (p1416). The T0 lanes represent samples taken of the protein 1L cultures prior to induction. The T24 lanes represent samples taken from the cultures after the overnight induction of 0.5 mM of IPTG. The protein ladder lane (MW) is labeled in kDa on the right. The expected band size of p1405 is 32.1 kDa. The expected band size of p1416 is 18.95 kDa. There is a distinct band at around the 36 kDa indicated yellow asterisk in the p1405, but not the p1416, assumed to be HSP23.5. The p1405 T24 shows a much thicker band at the same sized, indicated successful induction. The p1416 lanes show a distinct band between 17 and 28 kDa not present in the p1405 lanes (red star). However, there is no clear induction of ΔC-Hsp23.5 seen in the p1416 T24 lane.

(Figure 7). Protein at the expected size of 18.95 kDa was seen in the culture supernatant loaded on the column while no band of this size was detected in the flow-through or wash fractions. The

18.95 kDa band appeared again in the first elution fraction, confirming that the histidine tag of the protein interacted with the nickel column until it was eluted. After dialysis and cleavage of the HIS-SUMO tag, two distinct bands were present in the E2 fraction. The expected size of the cleaved, ΔC-HSP23.5 protein is 6.61 kDa and the expected size of the tag is 12.34 kDa. The lower band at approximately 6.61 kDa shows a slight separation into two possible bands. The higher band is located above 17 kDa and assumed to be the His-SUMO tag, which may migrate anomalously.

Previous purification attempts had revealed that the cleaved, ΔC-HSP23.5 remained bound to the nickel column after a second purification round through the nickel column (Appendix Figure 2). The isoelectric points (PIs) calculated for the His-SUMO tag, ΔC-HSP23.5, and the His-SUMO-ΔC-HSP23.5 are 5.7, 6.17 and 5.86, respectively. Due to the small difference in PI values, an ion exchange chromatography was performed in order to separate ΔC-HSP23.5 from the His-SUMO tag (Figure 8). Lanes 1-4 were samples of the fractions collected before NaCl concentration was increased in the buffer passing through the column. There are large distinct bands in these fractions located around 6.6 kDa, the expected size of ΔC-HSP23.5. Lanes 5-9 correspond to an increasing salt concentration in the chromatography buffer and each of these lanes contain various bands including the distinct band above the 17 kDa marker presumed to be the His-SUMO tag. Fractions from lanes 1-4 (total volume 10 mL) were collected and concentrated to 2 mL.

The concentration of the purified ΔC-HSP23.5 was determined using both BCA assays and SDS-PAGE analysis using both BSA and lysozyme as protein standards. A BCA assay with BSA as a standard reported a 0.98 mg/mL concentration. Lysozyme was also used as a protein standard as it has a closer molecular weight to the truncated protein. The BCA assay with lysozyme reported a 0.57 mg/mL concentration. An SDS gel was run with different volumes of

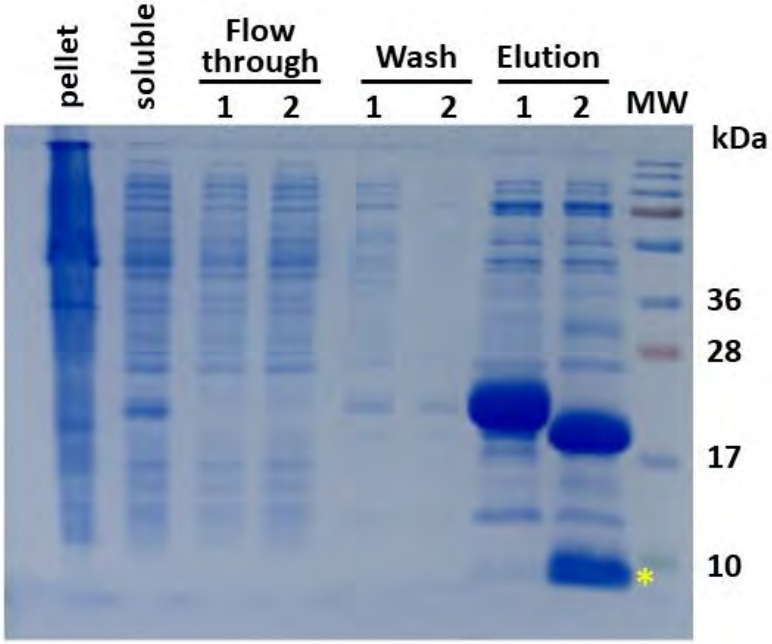

Figure 7: Purification and Cleavage of ΔC-Hsp23.5 using FPLC and a Nickel Resin. The lanes pellet, soluble, Flow-through 1 and 2, Wash 1 and 2, Elution 1 and 2. The cells expressing ΔC-Hsp23.5 were pelleted, then resuspended in lysis buffer and disrupted with a microfluidizer. The solution was centrifuged down. The samples of the supernatant (soluble) and pellet were taken. The supernatant was run through a nickel resin with an FPLC machine and the flow-through was collected. The column was washed with lysis buffer. And then eluted with elution buffer. The elution fraction was set up in a dialysis against 1x PBS and the His-SUMO tag was cleaved with an ULP1 protease (Elution 2). The tagged, truncated protein was expected to be 18.95 kDa. The cleaved truncated protein is expected to be 6.61 kDa. The cleaved tag is expected to be 12.34 kDa. The yellow asterisk indicates the ΔC-Hsp23.5 at 6.6 kDa.

p1416 and known amounts of lysozyme. A standard curve was calculated using ImageJ with lysozyme and the p1416 concentration yielded was 0.42 mg/mL (Table 1). However, given that BSA is commonly used as a standard protein and that a BCA assay is more sensitive, the expected protein concentration of purified ΔC-HSP23.5 was determined to be 0.98 mg/mL.

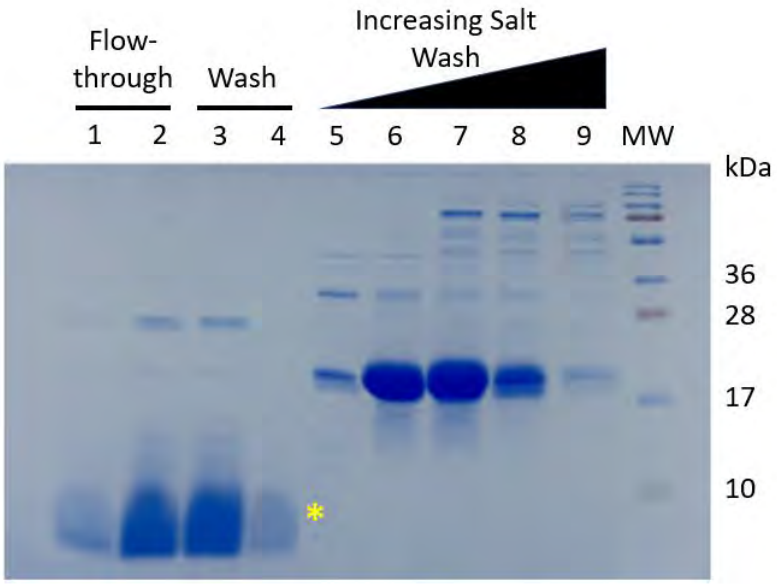

Figure 8: Ion exchange chromatography purification of ΔC-HSP23.5. The elution 2 fraction (See Figure 7) was used for ion exchange chromatography with an anion column that was washed with different concentrations of Buffer A and Buffer B. Buffer A was 20 mM Tris and Buffer B was 20 mM Tris and 1 M NaCl. Expected PI of HIS-SUMO-truncHSP23.5 is 5.86; Expected PI of HIS-SUMO tag is 5.7; and expected PI of ΔC-HSP23.5 is 6.17 Lanes 1-2 are the flow-through fraction. Lanes 2-4 are the fractions washed with 20 mM Tris. Lanes 5-9 are fractions washed with an increasing NaCl concentration. Lane MW corresponds to a protein ladder with kDa indicated to the right. Fractions were separated on an 18% SDS-PAGE and gel stained with Coomassie blue. The yellow asterisk indicates the 6.6 kDa ΔC-HSP23.5.

Table 1. The protein concentration determination of purified ΔC-Hsp23.5. The assays, BCA assays or an image J analysis of an SDS gel, used either Lysozyme or BSA as protein standards to determine the protein concentration of ΔC-Hsp23.5 in mg/mL.

Assay	Standard Protein	Concentration Determined (mg/mL)
BCA	BSA	0.98
BCA	Lysozyme	0.57
SDS gel Analysis	Lysozyme	0.42

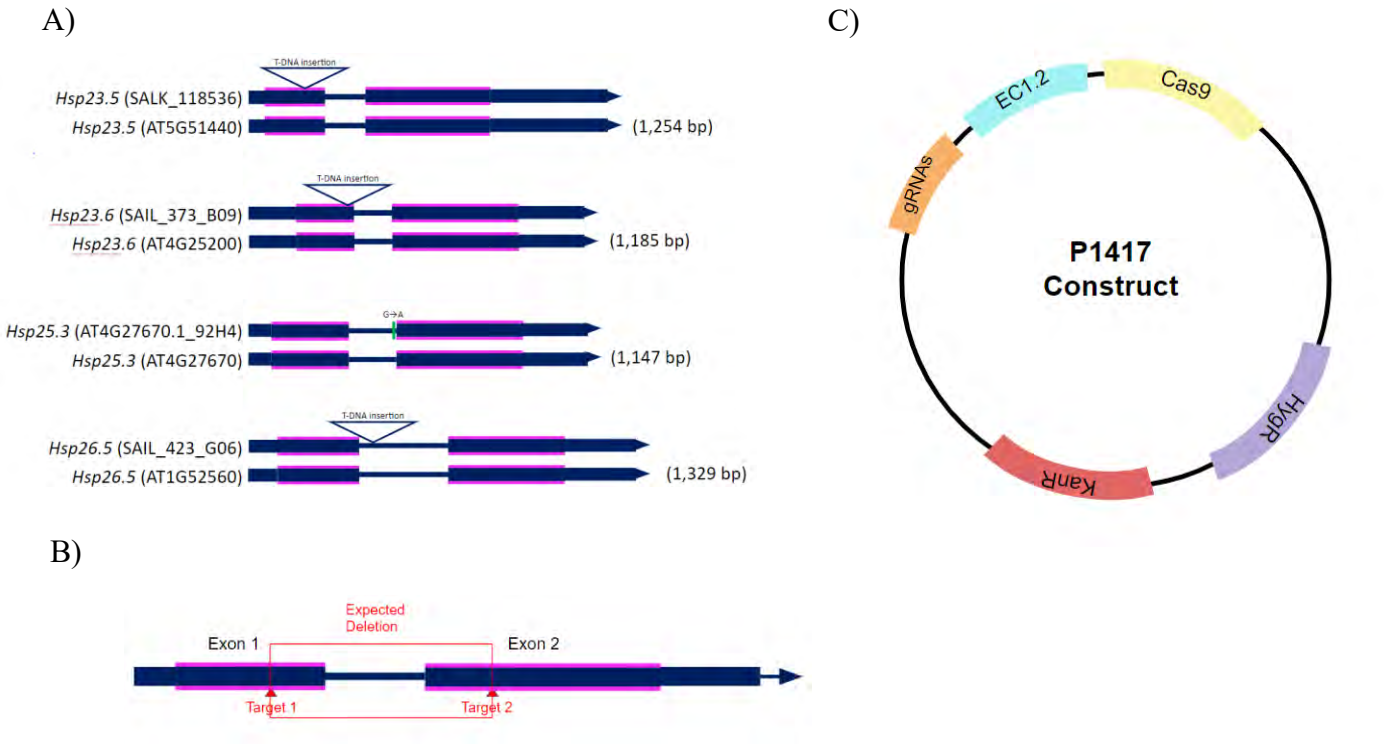

Figure 9: Diagram of the Four Organelle sHSP Mutants. A) Gene diagram of the four sHSP mutants in the Vierling Lab. HSP23.5, HSP23.6, and HSP26.5 have T-DNA insertions that generate null mutants in the Colombia background. The HSP25.3 gene has a point mutation to create a null mutant in the Landsberg background. The mutant genes (top) are compared to the normal genes (bottom). B) The proposed CRISPR/Cas9 HSP25.3 mutant in the Colombia background. The red arrows represent the gRNA targets, and the red box is the expected deletion size in the mutant. C) The CRISPR/Cas9 plasmid map of the genes transformed to generate a new HSP25.3 mutant. The construct contains the gRNAs with HSP25.3 target sequences, EC1.2 egg-cell promoter driving the Cas9 gene, and hygromycin and kanamycin resistance genes.

The Vierling Lab has mutants for each of the organelle sHSPs targeted to either the chloroplast or mitochondrion. However, the HSP25.3 mutant in the lab was created in the Landsberg accession and could potentially have a mix of Landsberg alleles (Figure 9A) Therefore, the aim in this part of my project was to create a second null mutant for the chloroplast HSP25.3 in the Colombia background of *A. thaliana*. A vector was designed using a CRISPR/Cas9 protocol to create a large deletion of 488 bp across two exons (Figure 9B). Two gRNAs containing target sequences of HSP25.3 (designed by Prem Patel) were cloned into a Cas9 construct using Golden Gate Cloning. The construct p1385 contained the gRNA scaffolding gene and was used as a template in a PCR reaction using the primers DT1-BsF, DT1-F0, DT2-R0, and DT2-BsR. These primers added in the Cas9 target sequences of HSP23.5 into

the vector in order to create the guide RNAs. The primers, DT1-BsF, DT1-F0, DT2-R0, and DT2-BsR, in the PCR reaction with the template p1385 yielded the expected 600 bp band on a 1% agarose TAE gel. The products were extracted from the agarose gel and used in the Golden Gate cloning to insert them into the vector p1384. P1384 was the destination vector containing the Cas9 gene, EC1.2 promoter, hygromycin-resistance gene, and kanamycin-resistance gene (Figure 9C). Cloning the guide RNAs (p1385) into the vector with the Cas9 gene (p1384) yielded the new product plasmid p1417. The products were then transformed into competent *E. coli* cells. A colony PCR was performed on seven different colonies (Figure 10). The expected size of the band using primers 357 and 358 would be approximately 730 bp. Clones 1, 2, 3, 4, 6 and 7 showed a band at the expected size compared to the 1 kb ladder. Clone 7 was further confirmed to contain the desired construct through sequencing.

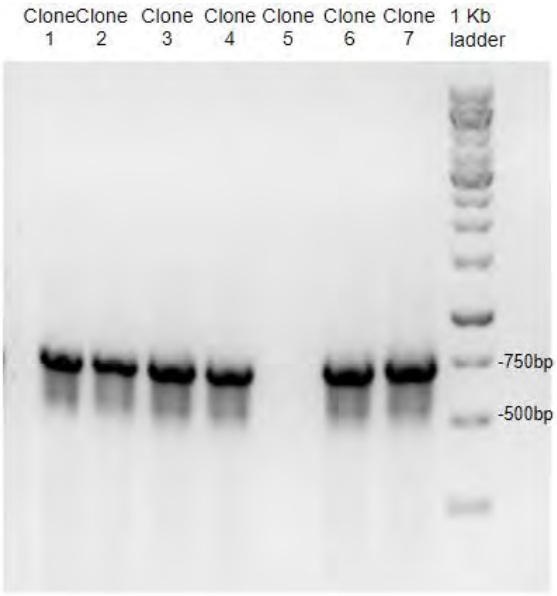

Figure 10: **Colony PCR of the golden gate cloning products of the Hsp25.3 CRISPR construct transformed into competent *E. coli* cells.** The primers 357 and 358 used in the colony PCR would yield an expected band size of 730 bp. Lanes 1-7 represent seven different colonies from the transformation compared to a 1 kb ladder. All of the clones, except #5, showed the expected band at approximately 730 bp. 1% agarose TAE gel with DNA stained using gel red.

The confirmed clone was then transformed into agrobacterium cells through electroporation. Colombia *A. thaliana* plants were floral dipped into the agrobacteria to take up the CRISPR/Cas9 plasmid. Plants were grown until mature and then harvested, yielding about ten thousand seeds. With help from current lab member Fabian Suri-Payer, around 8000 seeds were screened on hygromycin MS media plates using a hypocotyl elongation screening assay taken directly from Harrison et al., 2006. Currently, around 30 T1 plants are growing for genotyping.

sHSP-GFP Localization

Figure 11: The HSP-GFP Fusion Gene Constructs. Each of the four HSP genes with their native promoter were cloned to insert a GFP gene right before the endogenous stop codon of the sHSP. PP5 corresponds to HSP23.5-GFP, PP6 corresponds to HSP23.6-GFP, PP7 Corresponds to HSP25.3-GFP, and PP8 corresponds to HSP26.5-GFP. Plasmids were constructed by and introduced into *A. thaliana* by Parth Patel.

The organelle-localized sHSPs are predicted to localize to either the chloroplast, mitochondrion or both. Each of the sHSP genes of interest (HSP23.5, HSP23.6, HSP25.3, HSP26.5) with their native promoters were fused with a GFP gene directly before the stop codon (Figure 11). The constructs in Table 2 were transformed into two different backgrounds, Colombia (Col) and quadruple knock out (*qko*) mutant plants, resulting in 8 different transgenic lines. The Colombia background still contains the four wildtype sHSP genes of interest, while the *qko* background carries null mutations for all of these sHSPs. Lab member Parth Patel identified multiple T1 independent lines from each transformation and harvested the seeds. The seeds (T2 seeds) were plated on hygromycin by former lab member Tianxiang Liu. During the COVID shutdown, those plated seeds were left to stratify for a longer period of time than a normal 2-day period. After the shutdown was lifted, I took over the project during this step. The long stratification made the screening for a 3:1 ratio difficult in the seedlings as hygromycin does not completely stop growth of non-resistant plants. Three identified segregating lines per each construct in each background (Table 2) were identified and 10-12 plants each were transplanted. The long period of growth also resulted in death of many transplanted plants. The seeds from these plants were then screened for homozygous lines. Approximately 10-12 plants from each identified line were transferred to soil and harvested for T3 seeds. T3 seeds were screened on hygromycin to identify lines that showed 100% resistance and therefore would be homozygous for the sHSP-GFP transgene. Table 2 lists the number of confirmed homozygous T3 independent lines. The transgenic lines in the Col background were used for investigation of protein localization. There were 2 homozygous lines identified for HSP23.5-GFP (PP5), 4 for HSP23.6-GFP (PP6), 4 for HSP25.3-GFP (PP7), and 4 for HSP26.5-GFP (PP8) Col transgenic plants

(Table 3). At least two homozygous lines were also identified for each HSP-GFP gene in the *qko* background (Table 4).

Table 2. The HSP-GFP fusion constructs generated and transformed into two different genetic backgrounds, Col-Columbia, and *qko*-quadruple knockout of the four sHSPs and the independent lines identified for each generation. T2 lines listed segregated 3:1 for antibiotic resistance. T3 lines listed are homozygous for the transgene.

Construct	Promoter	Gene	Background	T1 Independent Lines	T2 Independent Lines	T3 Independent Lines
pPP5	-515 bp	HSP23.5-GFP	Col	10	3	2
			qko	~10	3	10
pPP6	-1141 bp	HSP23.6-GFP	Col	12	3	4
			qko	13	3	3
pPP7	-1225 bp	HSP25.3-GFP	Col	12	3	4
			qko	~10	3	2
pPP8	-2854 bp	HSP26.5-GFP	Col	~10	3	4
			qko	~10	3	5

Table 3. The identified HSP-GFP lines found in the Col background

Gene	Background	Homozygous Line
HSP23.5-GFP	Col	PP5.4.6_Col
HSP23.5-GFP	Col	PP5.5.5_Col
HSP23.6-GFP	Col	PP6.2.2_Col
HSP23.6-GFP	Col	PP6.2.5_Col
HSP23.6-GFP	Col	PP6.8.6_Col
HSP23.6-GFP	Col	PP6.9.6_Col
HSP25.3-GFP	Col	PP7.4.2_Col
HSP25.3-GFP	Col	PP7.4.6_Col
HSP25.3-GFP	Col	PP7.4.8_Col
HSP25.3-GFP	Col	PP7.12.1_Col
HSP26.5-GFP	Col	PP8.1.3_Col
HSP26.5-GFP	Col	PP8.1.4_Col
HSP26.5-GFP	Col	PP8.7.1_Col
HSP26.5-GFP	Col	PP8.7.4_Col

Table 4. The identified HSP-GFP homozygous lines found in the *qko* background

Gene	Background	Homozygous Line
HSP23.5-GFP	*qko*	PP5.5.1_QKO
HSP23.5-GFP	*qko*	PP5.5.5_QKO
HSP23.5-GFP	*qko*	PP5.5.8_QKO
HSP23.5-GFP	*qko*	PP5.5.10_QKO
HSP23.5-GFP	*qko*	PP5.7.6_QKO
HSP23.5-GFP	*qko*	PP5.7.7_QKO
HSP23.5-GFP	*qko*	PP5.7.9_QKO
HSP23.5-GFP	*qko*	PP5.7.11_QKO
HSP23.5-GFP	*qko*	PP5.7.12_QKO
HSP23.5-GFP	*qko*	PP5.9.4_QKO
HSP23.6-GFP	*qko*	PP6.5.1_QKO
HSP23.6-GFP	*qko*	PP6.5.6_QKO
HSP23.6-GFP	*qko*	PP6.12.3_QKO
HSP25.3-GFP	*qko*	PP7.3.2_QKO
HSP25.3-GFP	*qko*	PP7.3.6_QKO
HSP26.5-GFP	*qko*	PP8.5.7_QKO
HSP26.5-GFP	*qko*	PP8.7.4_QKO
HSP26.5-GFP	*qko*	PP8.8.2_QKO
HSP26.5-GFP	*qko*	PP8.8.3_QKO
HSP26.5-GFP	*qko*	PP8.8.5_QKO

One or more of the sHSP-GFP lines for each gene in each background were visualized for localization in either mitochondria and/or chloroplasts. The two sHSPs expected to dual-localize to both organelles (HSP23.5 and HSP23.6) were investigated to determine if they could be seen in both organelles by observing seedling roots and cotyledons. Figure 12 shows the localization of HSP23.5-GFP in root cells. Mitochondria were visualized in red by staining with MitoTracker. These sHSPs (visualized by GFP) are expected to only be visible after a heat treatment that induced expression. However, the HSP23.5-GFP fusion line was clearly visible in the RT seedlings. This was confirmed in two lines of HSP23.5-GFP in the Col background (PP5.5.5col and PP5.4.6col) and in one line of HSP23.5-GFP in the *qko* background (PP5.5.8qko). After heat treatment, the WT and Mito-GFP are similar in GFP detection and mitochondria or chloroplast visualization as compared to RT as expected. However, in both Col backgrounds, large aggregates formed. The *qko* background after heat treatment showed localization to the mitochondria similar to the same line with RT treatment. The HSP23.5-GFP fusion lines were also visualized in the chloroplasts in the cotyledons (Figure 13). The chloroplasts were visualized in red through auto-fluorescence. In both WT RT and WT heat-

treated leaves, there is no GFP present. GFP is detected at RT in all HSP23.5-GFP fusion lines. The amount of expression observed differs in each line. PP5.5.5col shows high GFP levels, while PP5.4.6col and PP5.5.8qko shows a lower GFP detection. In the heat-treated seedlings there is a consistent GFP level in all of the HSP23.5-GFP fusion lines. The HSP23.5-GFP protein (shown

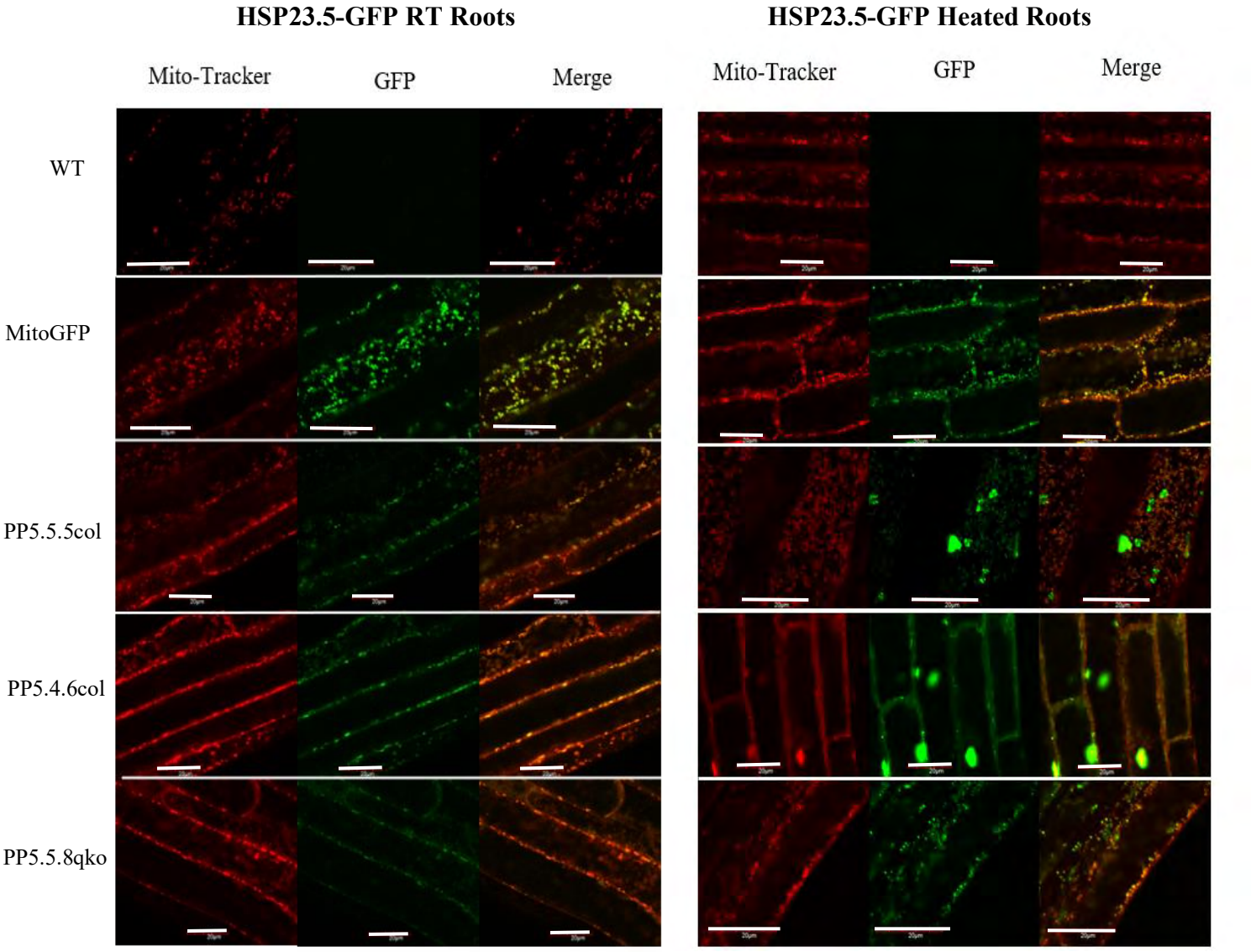

Figure 12: Localization of HSP23.5-GFP lines in Roots of *A. thaliana*. Seedlings were grown for 5-9 days until roots were long enough to observe. Seedlings were heat treated for 60 min at 38°C and observed after 90 min at room temperature (RT) (right). Seedlings at RT were also observed (left). Seedlings were stained with MitoTracker Orange for mitochondrial visualization in red (left columns). GFP was visualized in the middle columns in green. The right columns merge the MitoTracker and GFP signals. The roots were visualized in WT, MitoGFP, PP5.5.5col, PP5.4.6col, and PP5.5.8qko. White scale bars at the bottom of the images indicate 20 µm.

in green) does not merge with the chloroplasts as expected, but instead appears to surround the organelle.

The HSP23.6-GFP lines were observed under the same conditions in mitochondria and chloroplasts. The WT control is consistent in both roots and cotyledons with no GFP detected (Figure 14 and 15). The MitoGFP control also remains the same in roots for RT and heated samples. The HSP23.6-GFP lines were not expected to express protein at RT, but there is clear GFP detection in both root and leaf cells at RT (Figures 14 and 15). Both the HSP23.6-GFP lines in the Col background and HSP23.6-GFP line in the *qko* background show localization at RT (Figure 14), however the signal is lower in both Mito-Tracker and GFP detection compared to the WT and Mito-GFP controls. All the HSP23.6-GFP lines show localization in the heated root samples and yellow coloration in the merged column, indicated localization to mitochondria.

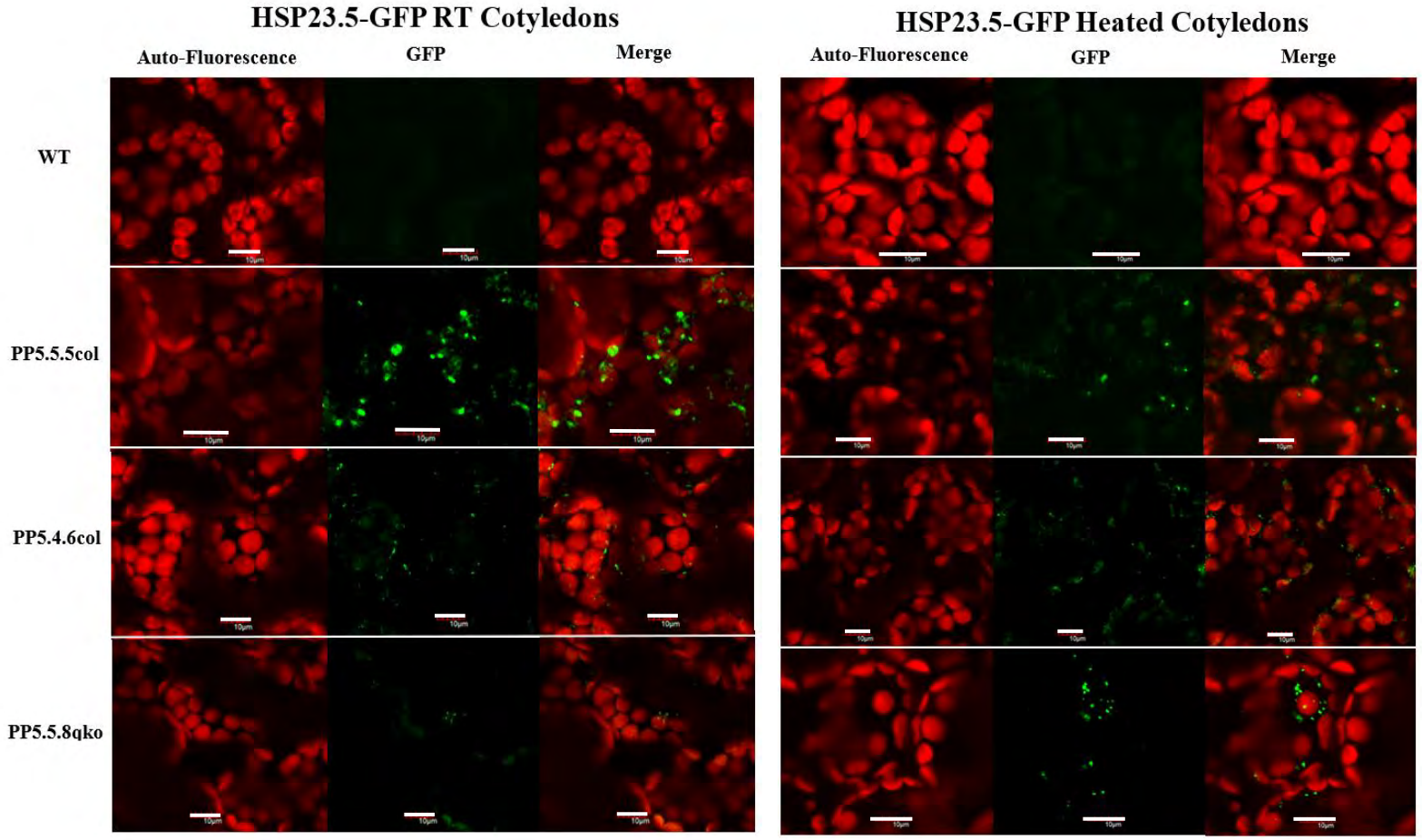

Figure 13: Localization of HSP23.5-GFP lines in cotyledons of *A. thaliana*. Seedlings were grown for 5-9 days until cotyledons were large enough to observe. Seedlings were heat treated for 60 min at 38°C and observed after 90 min (right). Seedlings at RT were also observed (left). Chloroplasts were observed through autofluorescence in red (left columns). GFP was visualized in the middle columns in green. The right columns are the merging of both autofluorescence and GFP. The roots were visualized in WT, PP5.5.5col, PP5.4.6col, and PP5.5.8qko. White scale bars at the bottom of the images indicate 10 µm.

However, all three transgenic lines also show some large aggregation of GFP that does not merge with the MitoTracker. GFP detection in the leaf cells at RT is similar in the PP6.2.5col and PP6.12.3qko lines (Figure 15). The PP6.2.2col line shows a higher GFP level in comparison. The GFP does not merge with the red auto-fluorescence and is dispersed throughout the sample. The heated leaf samples show an upregulation of GFP levels in the PP6.2.5col and PP6.12.3qko lines. The GFP level is relatively similar between the PP6.2.2col line at RT and heat-treated and the

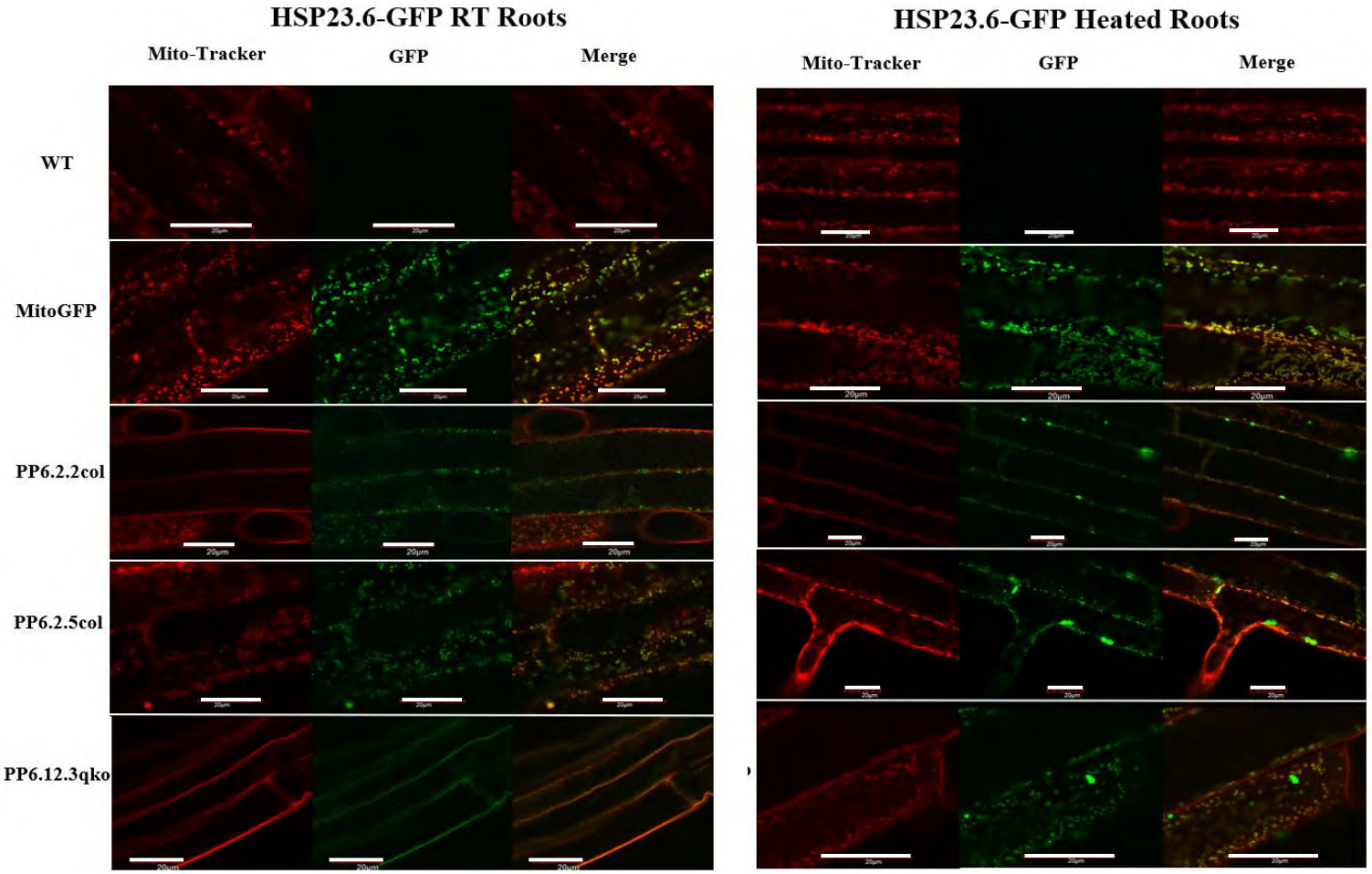

Figure 14: Localization of HSP23.6-GFP lines in Roots of *A. thaliana*. Seedlings were grown for 5-9 days until roots were long enough to observe. Seedlings were heat treated for 60 min at 38°C and observed after 90 min (right). Seedlings at RT were also observed (left). Seedlings were stained with MitoTracker Orange for mitochondria visualization in red (left columns). GFP was visualized in the middle columns in green. The right columns are the merging of both MitoTracker and GFP. The roots were visualized in WT, MitoGFP, PP6.2.2col, PP6.2.5col, and PP6.12.3qko. White scale bars at the bottom of the images indicate 20 µm.

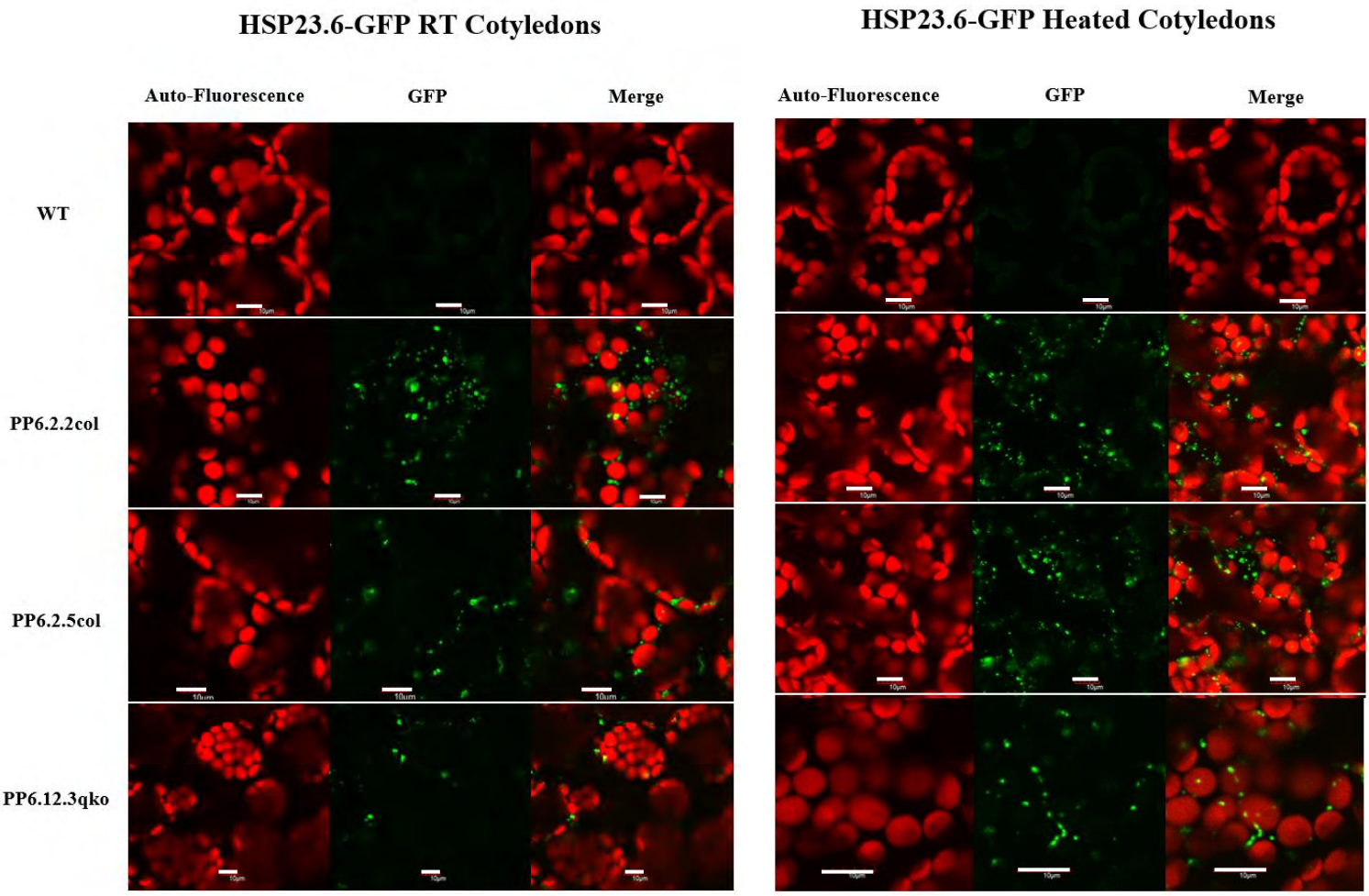

Figure 15: Localization of HSP23.6-GFP lines in cotyledons of *A. thaliana*. Seedlings were grown for 5-9 days until cotyledons were large enough to observe. Seedlings were heat treated for 60 min at 38°C and observed after 90 min (right). Seedlings at RT were also observed (left). Chloroplasts were observed through autofluorescence in red (left columns). GFP was visualized in the middle columns in green. The right columns are the merging of both autofluorescence and GFP. The roots were visualized in WT, PP6.2.2col, PP6.2.5col, and PP6.12.3qko. White scale bars at the bottom of the images indicate 10 µm.

GFP levels are relatively similar between the three transgenic lines in the heat-treated leaf samples.

The HSP25.3 protein is expected to localize to the chloroplast and was visualized in *A. thaliana* cotyledons (Figure 15). The WT control shows no GFP and only auto-fluorescence at both RT and heated treatments as expected. The HSP25.3 protein is not expected to be expressed at room temperature and there is no GFP detected in any of the HSP25.3-GFP fusion lines at RT.

Expression of HSP25.3-GFP was seen in the heated samples with GFP detected in two lines of HSP25.3-GFP in the Col background and one line of HSP25.3-GFP in the *qko* background. The strongest GFP signal was seen in the PP7.4.6col line, while the PP7.4.8col and PP7.3.2qko lines showed less GFP. There was no merge between the red auto-fluorescence and GFP in the heated PP7.4.6col and PP7.4.8col lines. The GFP surrounded the red chloroplasts in the heated merge column. There was some indication of localization to the chloroplasts seen in the PP7.3.2qko line. The heated merge pictures showed 2-3 areas with yellow coloration, suggesting the GFP localized with the chloroplasts in small amounts.

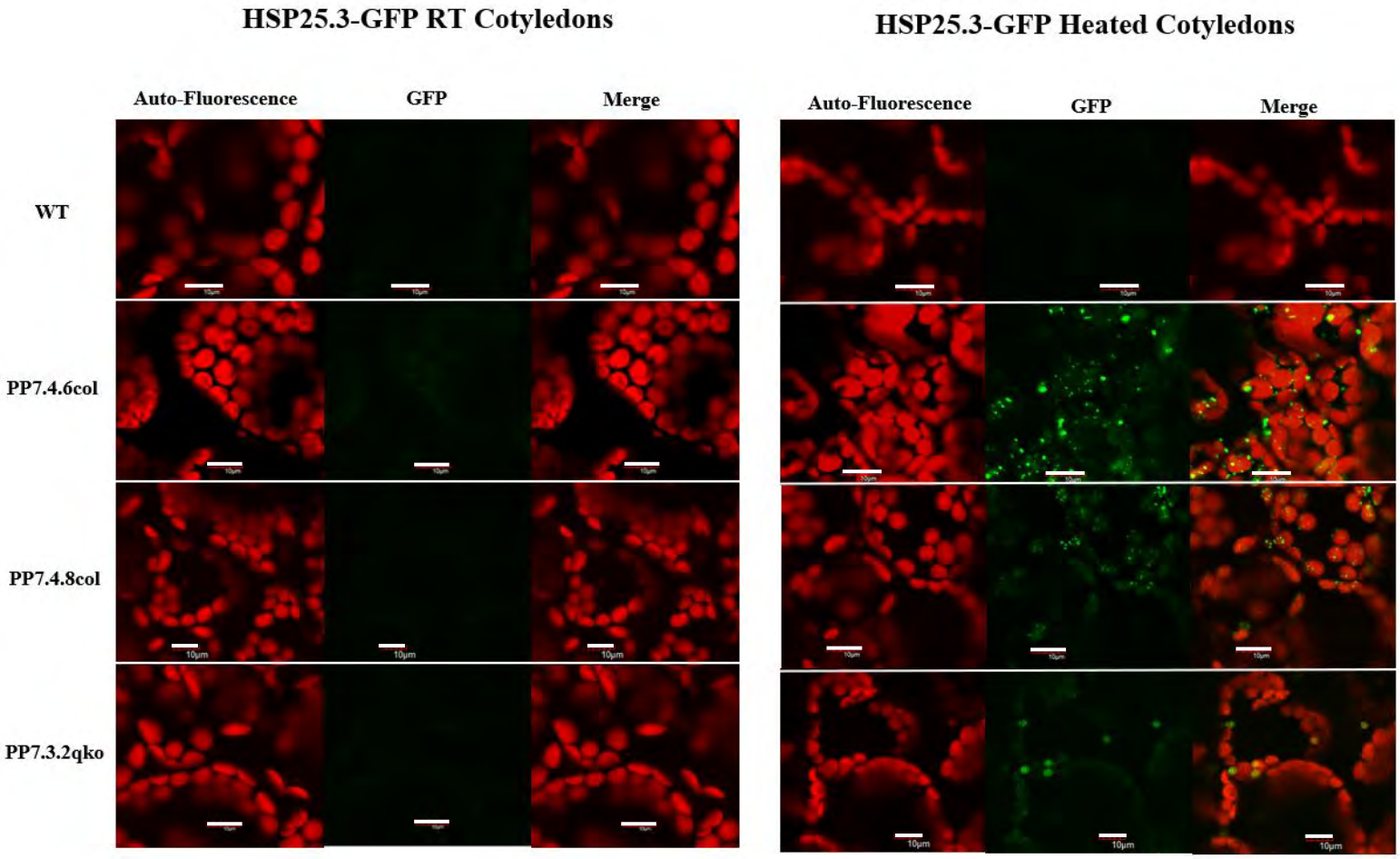

Figure 16: Localization of HSP25.3-GFP lines in Cotyledons of *A. thaliana*. Seedlings were grown for 5-9 days until cotyledons were large enough to observe. Seedlings were heat treated for 60 min at 38°C and observed after 90 min (right). Seedlings at RT were also observed (left). Chloroplasts were observed through autofluorescence in red (left columns). GFP was visualized in the middle columns in green. The right columns are the merging of both autofluorescence and GFP. The roots were visualized in WT, PP7.4.6col, PP7.4.8col, and PP7.3.2qko. White scale bars at the bottom of the images indicate 10 µm.

The HSP26.5 protein is expected to localize to the mitochondria. HSP26.5-GFP lines were visualized in roots (Figure 17). The WT control shows only red mitochondria stained with MitoTracker in both RT and heated seedlings. The MitoGFP controls shows both GFP and the MitoTracker merging in RT and heated samples as another control. HSP26.5 is not expected to be expressed at RT. The roots observed in RT seedlings detect no GFP in either of the two HSP26.5-GFP col lines (PP8.1.4col and PP8.7.1col) or the HSP-26.5-GFP *qko* line

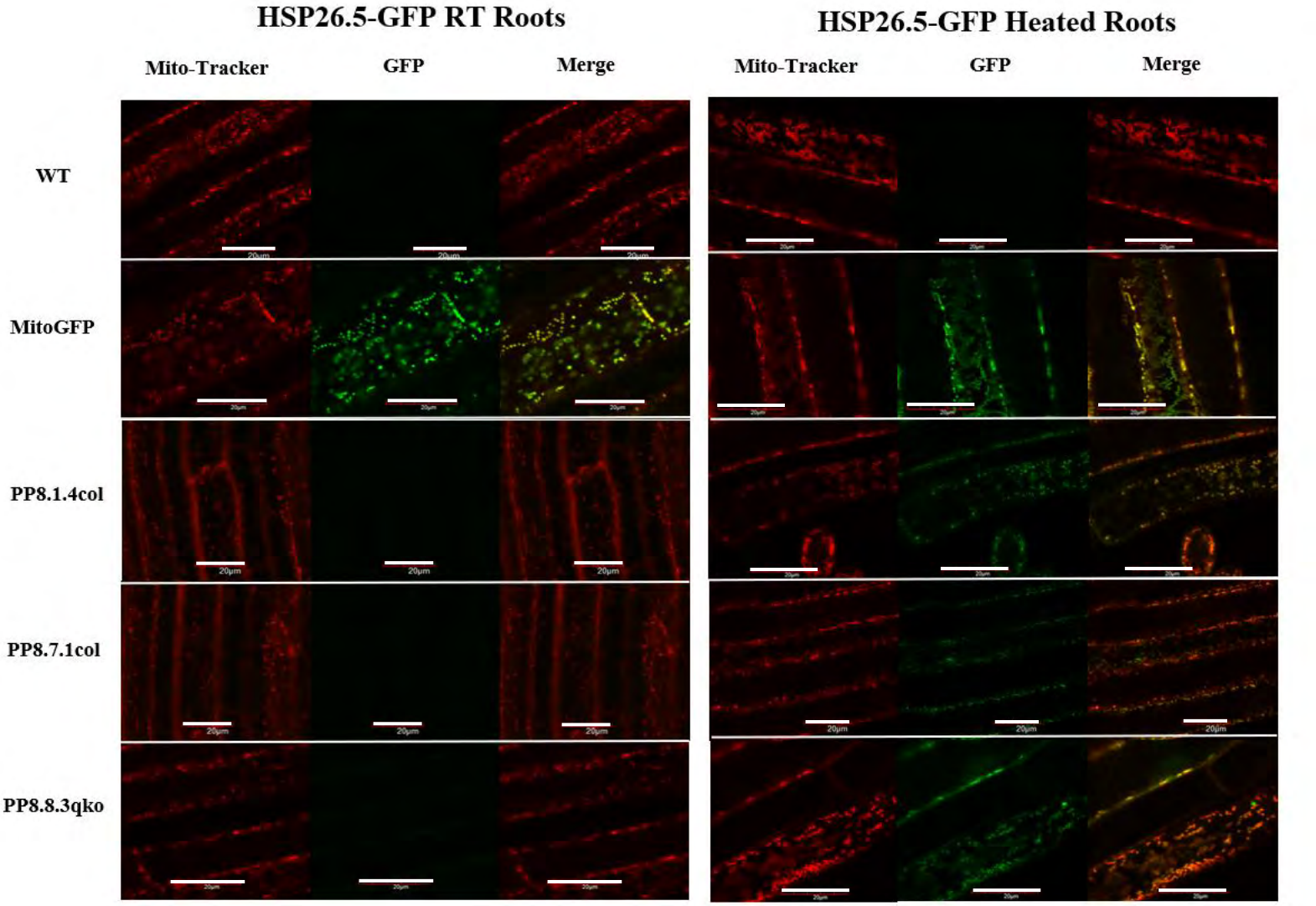

Figure 17: Localization of HSP26.5-GFP lines in Roots of *A. thaliana*. Seedlings were grown for 5-9 days until roots were long enough to observe. Seedlings were heat treated for 60 min at 38°C and observed after 90 min (right). Seedlings at RT were also observed (left). Seedlings were stained with MitoTracker Orange for mitochondria visualization in red (left columns). GFP was visualized in the middle columns in green. The right columns are the merging of both MitoTracker and GFP. The roots were visualized in WT, MitoGFP, PP8.1.4col, PP8.7.1col, and PP8.8.3qko. White scale bars at the bottom of the images indicate 20 µm.

(PP8.8.3qko). However, in the heated roots, there is GFP in all three of the transgenic lines. The GFP detected merges with the red MitoTracker to form a yellow coloration similar to the MitoGFP control, indicating localization to the mitochondria.

Generating Complementation Vectors for the sHSP mutants

The Vierling lab has mutants for the four organelle HSPs in *A. thaliana*. In order to prove that any phenotype observed in the mutants is occurring from the absence of sHSPs, complementation vectors that are able to reintroduce the wild type sHSP genes into the mutant background are needed to rescue that phenotype. Complementation vectors were generated for all four of the sHSPs (HSP23.5, HSP23.6, HSP25.3, and HSP26.5) from plasmids that contained each of the sHSP genes with a GFP gene added before the stop codon (See Figure 11). The HSP-GFP lines were used as backbones to generate complementation vectors for each of the sHSPs by amplifying the plasmid, removing the GFP gene, and adding in the stop codon, 3' UTR, and native terminator (Figure 18). For cloning I amplified three fragments in for each vector: A, B, and C. Fragment A in each of the complementation vectors was approximately 8000 bp.

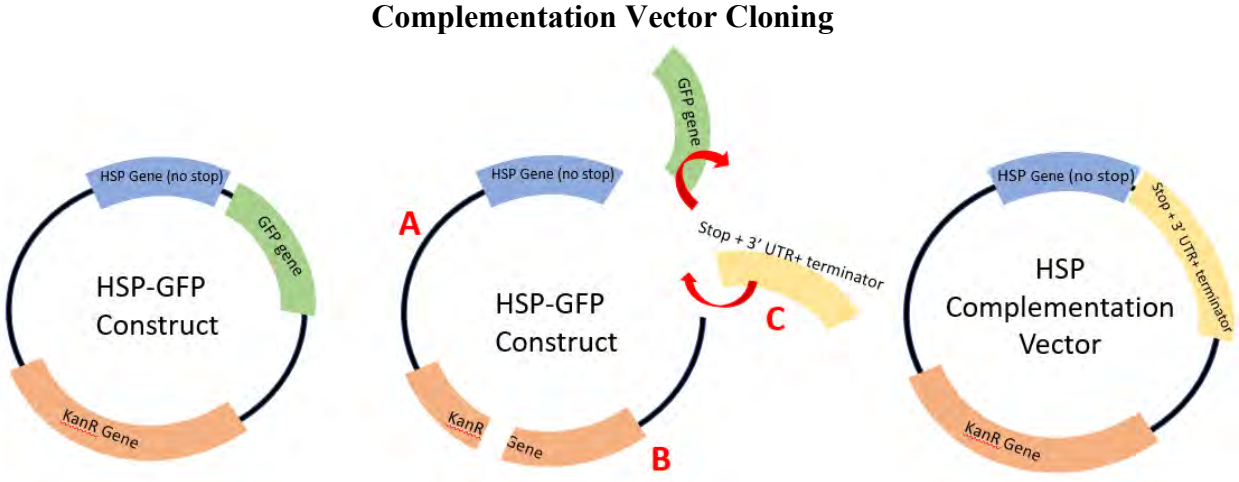

Figure 18: A Schematic Diagram of the HSP Complementation Cloning. This represents the flow chart of the cloning process for generating complementation vectors for each sHSP. The starting construct (far left) is one of the HSP-GFP plasmids which contains the Native HSP promoter, the HSP gene until the stop codon, and a kanamycin resistance gene. The plasmid backbone was amplified using two sets of primers to remove the GFP gene and break the plasmid into two fragments: A and B. The stop codon, 3' UTR, and native HSP terminator were amplified from genomic DNA to generate a third fragment: C (Middle). The three fragments were cloned together via Gibson Assembly to generate an HSP complementation vector containing the native HSP promoter, HSP gene, stop codon, 3' UTR, native terminator, and a kanamycin resistance gene (far right).

Fragment B was approximately 3000 bp and Fragment C was around 400-700bp. Each fragment contained Gibson Assembly overhangs to allow for the fragments to piece together during the Gibson Assembly Cloning.

HSP23.5 Complementation vector (p1425) was cloned from PP5 and WT genomic DNA. The PCR reaction amplifying fragment A from PP5 resulted in an expected 8000 bp band. The PCR reaction amplifying fragment B from PP5 resulted in a 3000 bp expected band size. The PCR reaction from WT DNA resulted in a 700 bp DNA band as expected for Fragment C. The expected bands were extracted from an agarose gel and used in a Gibson Assembly reaction to produce the HSP23.5 complementation vector p1425. After transformation into *E. coli*, colonies were grown on media plates containing kanamycin. The backbone of each complementation vector contained the kanamycin resistance gene. Therefore, the growth of colonies suggested successful generation and presence of p1425. However, a colony PCR with primers amplifying a portion of the HSP25.3 gene failed to result in any bands. Instead, a restriction digest was used to confirm the generation of p1425. The restriction enzyme EcoRV has three distinct cuts on both PP5 and p1425 predicted to generate three fragments at 1300, 2600, and 7000 bp. The restriction digest of four colonies resulted in three bands at the expected sizes on an agarose gel. The bands were identical to the control digest on PP5. This confirmed that a plasmid was generated, however since the control plasmids and new plasmid have the same cut sites, sequencing of the DNA would be needed to confirm the new p1425 plasmid.

HSP23.6 complementation vector (p1426) was cloned from PP6 and WT genomic DNA. The PCR reactions cloning fragments A and B from the plasmid backbone of PP6 resulted in the expected 8000 and 3000 bp bands on an agarose gel. However, the PCR reaction amplifying the portion of the HSP23.6 gene from genomic DNA with Gibson Assembly overhangs resulted in no product. Therefore, a PCR reaction was attempted to amplify only the genomic region of the HSP23.6 gene first. This resulted in an expected 400 bp band on an agarose gel. The DNA was extracted and used as a template in another PCR reaction to add the Gibson Assembly overhang extensions. The second PCR reaction resulted in a large band again around 400 bp, indicating the genomic DNA was successfully amplified with Gibson Assembly overhangs. DNA from each of the fragments was used in the Gibson Assembly cloning to attach the fragments together and generate HSP23.6 complementation vector p1426. The cloned products were transformed into *E. coli* and grown on plates with kanamycin. Several colonies grew on the plates, indicating the presence of the kanamycin resistance gene in these colonies and the generation of p1426. Colonies were further confirmed in a colony PCR amplifying a portion of theHSP23.6 gene from the clone DNA. Three clones yielded a 400 bp band on an agarose gel which was the expected amount of HSP23.6 DNA amplified. This further confirmed the generation of the HSP23.6 complementation vector (p1426).

HSP25.3 complementation vector (p1427) was cloned from PP7 and WT genomic DNA. The PCR reaction to amplify Fragment A from PP7 DNA yielded an expected 8000 bp band on an agarose gel. The PCR reaction to amplify Fragment B from PP7 DNA resulted in a 3000 bp band on an agarose gel. However, the PCR reaction to amplify Fragment C from genomic DNA resulted in no bands. A PCR amplification was attempted again using primers that only bind to the HSP 25.3 gene from genomic DNA and do not include the Gibson Assembly overhang. This PCR resulted in a band at the expected 700 bp on an agarose gel. The DNA was extracted from each of the fragments. Then, another PCR amplification was completed on the fragment C DNA in order to add in the Gibson Assembly overhang. This resulted in the expected 700 bp band on an agarose gel and was extracted for DNA. The Fragments were cloned together in a Gibson

Assembly cloning reaction to generate the HSP25.3 complementation vector p1427. The p1427 was transformed into *E. coli* and grown on plates with the antibiotic kanamycin. Colonies grown on the plates indicated the presence of the kanamycin resistance gene and there for the presence of p1427 that contains this gene. The clones were further confirmed through colony PCR by amplifying a portion of the HSP25.3 gene. Three clones resulted in the expected 400 bp band from the colony PCR, indicating the generation of p1427.

HSP26.5 complementation vector (p1428) was cloned from PP8 and WT genomic DNA. Fragments A and B were amplified using PP8 as the backbone using PCR. An agarose gel of the PCR products showed the expected 8000 bp and 3000 bp bands for Fragments A and B, respectively. A PCR was attempted to amplify Fragment C from WT genomic DNA, but no bands were present on an agarose gel compared to the expected 700 bp. A separate PCR was attempted amplifying only the region of DNA from the HSP26.5 gene and lacked the Gibson Assembly overhangs. This PCR product showed the expected 700 bp band on an agarose gel. The DNA was then extracted from each of the Fragments. The Gibson Assembly overhangs were added onto the DNA in Fragment C through another PCR using Fragment C DNA as a template. This agarose gel resulted in the expected 700 bp. The DNA was then extracted from the agarose gel. The DNA from Fragments A, B, and C were used in a Gibson assembly cloning reaction to generate p1428. The p1428 was then transformed into *E. coli* and grown on plates with kanamycin. Colony growth indicated the presence of p1428 which contained the kanamycin resistant gene. One colony grew on the antibiotic plates and was used in a colony PCR that amplified a portion of the HSP26.5 gene. The amplification expected a 700 bp band, but instead no bands were present on an agarose gel. Instead, a restriction digest was completed with the restriction enzyme XbaI. This restriction enzyme has 3 cut sites in the p1428 construct at 600 bp, 3000 bp, and 10000 bp. As a control the restriction enzyme has the same cut sites resulting on the same bp sizes of the PP8 construct. The restriction digest confirmed one p1428 clone which had the three bands at the expected band sizes and was identical to the restriction digest performed on PP8. This suggested conformation of the generation of the HSP26.5 complementation vector p1428, however sequencing would further confirm the generation of the new plasmid.

Heat Stress Assays of sHSP mutants

As sHSPs are predicted to contribute to the first response to environmental stress, different heat stress assays have been completed on sHSP mutants in the Vierling lab. Preliminary data have indicated that heat stress may have an effect on seed setting in *A. thaliana*. In order to test the effect of heat stress on seed setting in sHSP mutants, first the optimal temperature that effects wild-type plants needed to be determined. *A. thaliana* WT plants were allowed to grow until several siliques had matured (were full length).

A

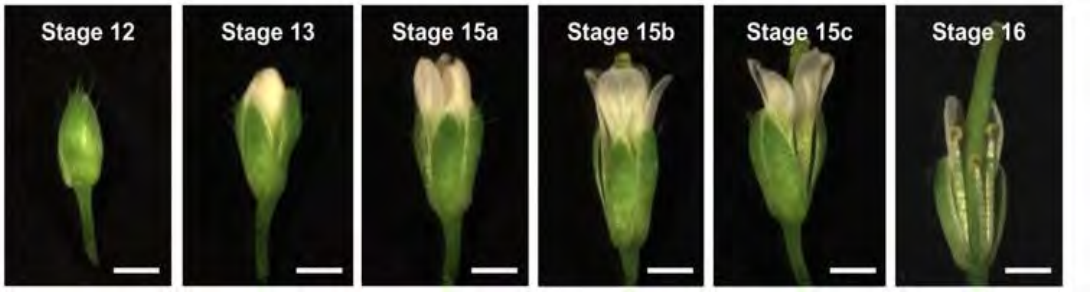

B

Figure 19: The Flowering Stages of *A. thaliana.* A) The developmental stages of flowering in *A. thaliana*. From Cai and Lashbrook, 2008. B) A marked flower with red thread in early stage 15 of flowering developmental stage before heat stress.

A

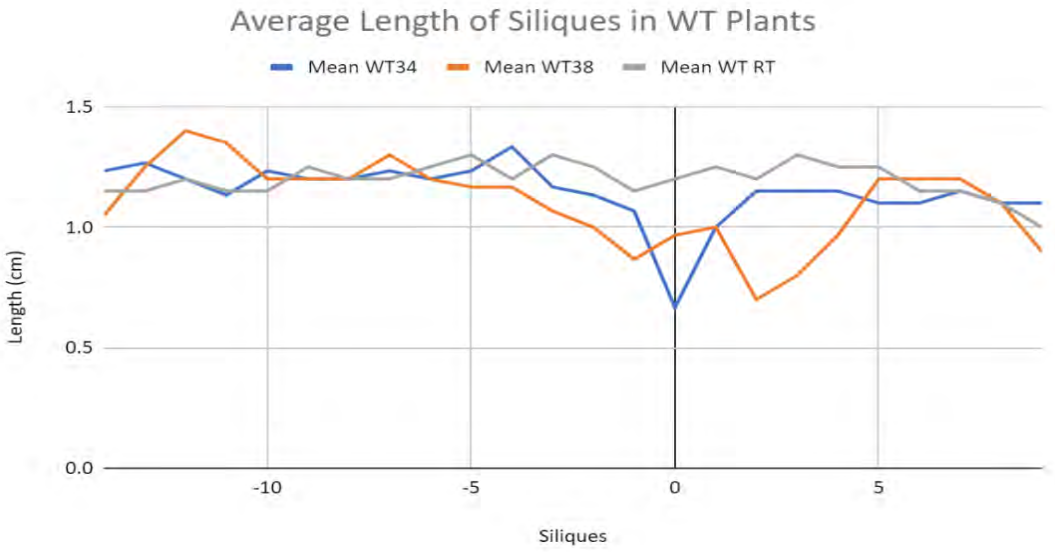

B

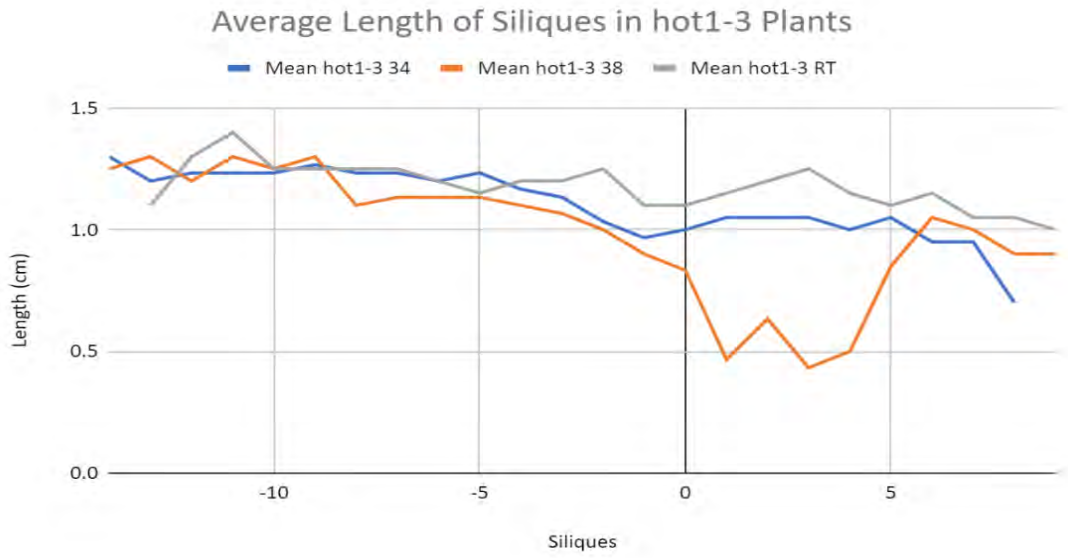

Figure 20: The Average Length of Siliques Before and After Heat Stress Treatment. WT and *hot1*-3 plants were grown until at least five siliques were mature and then a flower was marked on each of the plants. The plants were heat treated for 6 hrs over 2 days at either 34°C, 38°TC, or RT. The siliques that were fully matured prior to the heat stress and were below the marked silique in red thread were given a value below zero. Then counting up, the marked silique with red thread was indicated as silique "0" and the siliques that matured after the heat treatment were positive values. A) The graph of the silique measurement in cm of WT plants. The blue line indicates the average silique length of the 34°C heat treated WT plants. The orange line indicates the average silique length of the 38°C heat treated WT plants. The grey line indicated the average silique length of WT plants at RT. B) The graph of the silique measurement in cm of *hot1-3* heat treated plants. The coloring scheme from the WT graph indicating the temperature treatment is the same.

Additionally, *hot1-3* plants, which are null mutants for the HSP101 molecular chaperone and are known to be heat-sensitive, were also grown. After at least five siliques were matured, a flower in stage 12 to early stage 15 development was marked with red thread in 8 WT plants and 8 *hot1-3* plants (Figure 19). Earlier developmental stages were targeted to be marked (stage12-13), however some flowers in early stage 15 were also marked. This is the developmental stage in *A. thaliana* where the petals begin to show in the flower bud. Three plants of each genotype were then heat stressed for 6 hrs over 2 days at either 34°C or 38°C in a dark incubator. Two plants of each genotype were kept in the dark at room temperature during the treatment time as controls. The heat stress period took place 4 hrs into the 16 hr day light cycle. The plants were then returned to grow under normal conditions. After 10 days, the siliques from each plant were cut and measured (Figure 20). In Figure 20, the siliques that were fully matured prior to the heat stress and were below the marked silique in red thread were given a value below zero while the lowest number corresponds to the first matured silique. The marked silique with red thread was indicated as silique "0" and the siliques that matured after the heat treatment were marked in numerical order matching the position on the plant. The average silique measurement at the same position was averaged in each of the three plants per heat treatment and each of the two plants kept at RT. Figure 20A shows the RT siliques had a consistent silique length in WT plants. However, the average silique length when heat treated at 34°C shows a reduction in average length at silique 0, but then quickly returns to similar silique measurements as the RT. The average 38°C treated WT plants show a consistent reduction in silique length both before and after silique 0. In comparison to the *hot1-3* plants, the plants at RT and 34°C both have consistent and normal silique length throughout the heat stress assay (Figure 20B). However, the *hot1-3* siliques heat treated at 38°C showed a dramatic reduction in silique length after the marked silique (silique 0).

Discussion and Conclusions

Creating an antibody that recognizes HSP23.5

The Vierling lab already has antibodies against HSP23.6, HSP25.3, and HSP26.5, but in order to also detect expression of HSP23.5 efforts were undertaken to produce an antibody specific to this protein. This would complete the set of antibodies against the four organelle-localized sHSPs and allow quantitation of their expression and confirmation that the mutants are null for protein expression. HSP23.5 and HSP23.6 are very similar proteins, sharing a 66% identity and 77% similarity (Figure 5). The N-terminal domain is the most divergent, so by introducing an early stop codon in the HSP23.5 N-terminus and utilizing the resultant truncated proteins, it would be predicted to produce antibodies more specific to HSP23.5 than HSP23.6. An alignment of the part of the HSP23.5 N-terminal sequence chosen against the corresponding region of HSP23.6 showed a lower identity (52%) and similarity (66%) compared to the full-length protein. The portion of the protein that was truncated, which was mostly the ACD and CTD domain, had a protein sequence identity of 75% and similarity of 87% compared to the ACD and CTD of HSP23.6 (Appendix: Figure 1). However, there still is a possibility that an antibody that recognizes this segment of HSP23.5 will also recognize HSP23.6, but cross reactivity can be tested against the purified proteins and verified by immunoblotting with the corresponding sHSP mutants.

The ΔC-HSP23.5 protein (p1416) was the most critical for antibody generation, and this protein was purified and cleaved to remove the HIS-SUMO tag. The results from the first purification step using nickel chromatography indicate that the tagged and truncated protein was successfully obtained. Ion exchange chromatography was then needed to separate the affinity tag from the ΔC-HSP23.5 protein. In previous purification attempts, the cleaved ΔC-HSP23.5 protein and tag were loaded through the same nickel column. The affinity tag with the 6x histidine was expected to remain bound to the column while the ΔC-HSP23.5 protein would pass through to achieve purification and isolation of the ΔC-HSP23.5 protein. However, both the ΔC-HSP23.5 protein and the affinity tag remained bound to the nickel column until eluted with elution buffer (Appendix Figure 2). A low concentration of imidazole also proved to not disrupt ΔC-HSP23.5 interacting with the nickel column (data not shown). Instead, ion exchange chromatography was able to separate the ΔC-HSP23.5 protein from the tag based on the slight difference of PI values. An attempt to isolate the full length HSP23.5 protein (p1405) resulted in purification using only nickel affinity chromatography (Appendix Figure 3). It may be possible that the ΔC-HSP23.5 protein, due to being truncated, had exposed residues that would be sequestered in the full-length protein. These exposed residues in the ΔC-HSP23.5 protein could be causing an interaction with the nickel column even after the removal of the affinity tag that is not seen in the full-length protein.

The protein concentration was measured by two different methods, yielding different estimates. A Bradford assay was first used to measure purified ΔC-HSP23.5 protein concentration. However, the color development of a Bradford assay depends on the presence of arginine, lysine, and histidine. Therefore, a BCA assay was performed as one of the assays to measure the protein concentration. The BCA assay measures protein concentration based on peptide bonds and therefore should be independent of amino acid composition. Two standards were used: lysozyme and BSA. BSA is a commonly used protein standard, but has a molecular weight of around 66 kDa, while ΔC-HSP23.5 is only around 6.6 kDa. Lysozyme has a closer molecular weight of 14 kDa and therefore was also used as a standard. Table 1 summarized the three different protein concentration determinations for ΔC-Hsp23.5. The BSA standard reported a higher ΔC-HSP23.5 concentration of 0.98 mg/mL and the lysozyme reported a much lower concentration of 0.57 mg/mL (Table 1). An SDS gel was also run with lysozyme as a standard and a different amount of ΔC-HSP23.5. Image J analysis calculated a lowest ΔC-HSP23.5 concentration of 0.42 mg/mL (Table 1). However, given that BSA is a commonly used standard and that the higher protein concentration would more accurately represent the amount of protein shown in the SDS gel (Figure 7), the ΔC-HSP23.5 is most likely assumed to be closer to the 0.98 mg/mL concentration. The protein has been sent out for antibody production to Agrisera in Sweden, and the next step would be to test the antibody for specificity when it is available.

Creating CRISPR/cas9 HSP25.3 Mutant

The Vierling Lab has a HSP25.3 mutant in the Landsberg plant background that was generated by EMS mutagenesis. It has a point mutation in the 3'splice site (Figure 9) and results in a protein null. Although it has been crossed several times with Col background plants, there still may be residual Landsberg alleles in this mutant as well as other EMS mutations. The Landsberg background may respond differently to environmental stresses compared to the Col background. Therefore, in order to effectively analyze phenotypes caused by the lack of this sHSP and not by other factors, I sought to generate an HSP25.3 in the Col background suing CRISPR/Cas9. Target sequencing of the HSP25.3 gene were identified in exon 1 and 2 to be

cloned into guide RNAs and eventually into a plasmid containing an egg cell promoter, E.C1.2 and a Cas9 gene. The target sequences were designed to generate a null mutant by deleting portions of both exons. However, the expected deletion size from these target sequences is rather large at 488 bp. It is possible that the large deletion will not occur. It may also be possible that smaller deletions could occur that also result in a null mutant. The construct was confirmed through colony PCR and sequencing, and currently the T1 plants are growing and being genotyped by Fabian Suri-Payer. However, once homozygous lines for a null gene deletion have been identified, it is possible that the Cas9 protein may have off-targets. To eliminate the the Cas9 protein and the possibility of off-targets mutations, the HSP25.3 mutant should be backcrossed against wild-type plants to remove the Cas9 gene and guide RNAs.

HSP-GFP Localization

HSP25.3 and HSP26.5 are known to localize to the chloroplast ant mitochondrion, respectively. However, the localization of HSP23.5 and HSP23.6 is only predicted to both organelles and requires further analysis. To investigate the localization of these four proteins, HSP-GFP fusion lines were generated. The HSP-GFP fusion constructs were successfully transformed into Col and *qko* plants by former lab member Parth Patel. Harvested seeds taken from these plants were screened on hygromycin until homozygous lines were found. Four independent T3 lines were found in each of the transgenic Columbia background lines, except for PP5 (HSP23.5-GFP), which had only 2 identified homozygous lines. It is possible that one independent line may behave differently, and confirmation of localization can be indicated by visualizing the same results in at least two independent lines of the same HSP in the same background. Two each of the sHSP-GFP lines were visualized in the Col background, however only one line in the *qko* background was visualized. The GFP gene is longer in comparison to the short sHSP genes, so there was a concern that these HSP-GFP proteins would not localize properly in vivo. However, the GFP was tagged on the C-terminus of the gene and should not affect the transit peptide on the N-terminus. Additionally, sHSPs are typically favored in oligomeric state and then become upregulated and in response to stresses and become favored in a dimer state. It is possible that large GFP attached to the sHSPs affect the dimerization and/or oligomerization and that formation of higher order structures in the cytosol could inhibit transport into the organelles.

sHSPs are not typically expressed at room-temperature and are induced due to environmental stress such a heat stress. Therefore, it was expected that GFP fluorescence would not be detected in each of the sHSP-GFP fusion lines at room temperature. However, Figure 4 indicated that RNA levels of HSP23.5 can be detected at room temperature. Based off the controls of the heat map in Figure 4, it could be expected to see HSP23.5-GFP at room temperature, especially in roots.

In the HSP23.5-GFP fusion line the GFP fluorescence merged with the Mito-Tracker orange to appear yellow, indicating that the HSP23.5-GFP protein was localizing to the mitochondria in roots for both room temperature and heat-treated seedlings. However, the heat-treated seedlings also have large GFP aggregates. These large regions of fluorescence seen in Figure 12 could be due to the protein aggregating from the heat treatment. However, this GFP aggregation is not seen in the HSP23.5-GFP *qko* line. This could be an indication that the plant works and responds differently to heat stress when there are no organelle sHSPs. The HSP23.5-GFP lines are also expressing protein at both RT and heat treatments in leaves. There are no large GFP aggregates seen in the heat-treated Col background lines in leaves. The GFP is

dispersed in both temperature treatments and does not merge with the chlorophyll autofluorescence, indicating the HSP23.5-GFP protein is not localizing to chloroplasts in cotyledons. It appears that some of the GFP signal is surrounding some of the chloroplasts in the merged data.

Interestingly, GFP is detected in the HSP23.6-GFP lines at RT and in heated roots and leaves (Figure 14 and 15). The RT roots of the transgenic lines show GFP signal that merges with MitoTracker, indicating that HSP23.6-GFP localizes to mitochondria, even at RT (Figure 14). Additionally, RT cotyledons showed HSP23.6-GFP expression. However, there were no data indicating that this protein would be expressed. Little to no RNA levels were detected in shoots and leaves for HSP23.6 at RT (Figure 4). A western blot using antibodies against HSP23.5 and HSP23.6 could be used on RT and heated HSP-GFP lines to confirm these expression patterns. Interestingly, there are GFP aggregates present in the heat-treated HSP23.6-GFP root samples. This is similar to the HSP23.5-GFP heated roots, except here the HSP23.6-GFP *qko* line shows GFP aggregation as well. More lines in the *qko* background would need to be observed to confirm any indicated pattern. The GFP amount looks consistent between the RT and heated lines, with a slight possibility of more GFP detection in the heated leaves. This could indicate an up-regulation when exposed to heat treatment. Although localization in the chloroplasts is not seen in heated or RT leaves.

The HSP25.3 protein is known to localize to the chloroplast. The cotyledons of HSP25.3-GFP fusion lines were visualized with a confocal microscope (Figure 16). HSP25.3 is not known to be expressed at RT and therefore HSP25.3-GFP lines were not expected to express GFP. There was no GFP detected at RT in the leaves of HSP25.3-GFP col and HSP25.3-GFP *qko* seedlings, indicating that the HSP25.3-GFP protein was not expressed. The heat-treated leaves of the transgenic lines showed GFP in all three of the transgenic lines. This indicated an upregulation from the heat stress treatment. There was a strong detection of GFP in one of the col backgrounds and a slightly weaker detection in the second col background line. The weakest GFP signal was in the *qko* background, indicating not as much HSP25.3-GFP protein was expressed. There was still no merging of the green GFP and red auto-fluorescence, indicating that HSP25.3-GFP does not localize inside the chloroplast. The GFP was not as dispersed as seen in the leaves of the HSP23.5-GFP and HSP23.6-GFP lines. Instead, the GFP seems to surround the chloroplasts in the heated samples. It may be that the GFP protein attached to the sHSP affects the import into the organelle. It is also possible that the heat stress applied to the seedlings is enough to block protein transport. Since the localization to chloroplasts could not be confirmed in HSP25.3-GFP lines, it should not be a definitive conclusion that HSP23.5 and HSP23.6 GFP lines do not localize to the chloroplasts. Additionally, it seems that there are small yellow colorations in the PP7.3.2qko heated leaf. This may indicate that HSP25.3-GFP is able to localize to the chloroplast in *qko* backgrounds but not in Col. However, it seems that this is limited to localization to smaller chloroplasts and less protein expression. Figure 4 indicated RNA expression of HSP25.3 in roots in response to heat stress. However, HSP25.3-GFP lines were not visualized in roots for this project.

The HSP26.5 protein is expected to localize to the mitochondria and is not expected to be expressed at RT. Therefore, the HSP26.5-GFP proteins is expected to localize to the mitochondria in only heat-treated seedlings. The roots were observed in HSP26.5-GFP lines at RT and heated treatments (Figure 17). There was no GFP detected in any of the HSP26.5-GFP transgenic lines at RT as expected, indicating that HSP26.5-GFP was not expressed at RT regardless of the genotype background. The heat-treated roots then showed GFP detection in all

three of the transgenic lines (PP8.1.4col, PP8.7.1col, and PP8.8.3). The GFP and the Mito-Tracker merged to produce a yellow coloration, indicated the HSP26.5-GFP proteins are expressed after heat treatment and localize to the mitochondria in roots. HSP26.5-GFP lines were also visualized in leaves at both RT and heat-treated conditions (data not shown). There was no GFP protein seen at either condition in the Col backgrounds, however constant expression of HSP26.5-GFP was seen in one *qko* line in both conditions. More lines need to be visualized to confirm these results. Figure 4 indicates RNA levels of HSP26.5 in shoots in response to heat stress, so it may be that HSP26.5-GFP is expressed in roots.

Generating Complementation vectors for the sHSP mutants

The starting plasmid contained the HSP native promoter, HSP gene until the stop codon, a GFP gene, and a kanamycin resistance gene (Figure 18). In each of the HSP-GFP lines, the plasmid backbone was amplified to remove the GFP gene and insert the remainder of the HSP gene to generate complementation vectors. These complementation vectors will be critical in rescuing mutant phenotypes and contributing to researching the role of these sHSPs. The native terminator for each of the sHSPs was not known and was assumed when cloning up to 1 kb after the 3' UTR. There could be a possibility that the native terminator is not found within this region or may be cut off during the cloning process. The vectors were confirmed through colony PCR and restriction digests. However, both restriction digests on p1425 and p1428 clones have the same cut sites as the starting plasmids. Therefore, it is a possibility the plasmid generated is no different from the starting HSP-GFP vector. A sequencing alignment was able to confirm p1427 clones using Benchling software. However, the sequencing results from the other generated clones was inconclusive. It is most likely the primers used were insufficient for sequencing and new primers need to be designed for further sequencing.

Heat Stress Assays on sHSP mutants

The sHSPs are predicted to be the first response to heat stress in plants. Therefore, it is predicted that null mutants of sHSPs will have phenotypes when exposed to heat stress compared to WT plants. Preliminary data from the Vierling lab indicated that heat stress affects seed set in *A. thaliana.* Previous heat stress assays performed on these sHSP organelle mutants in the Vierling lab showed no strong phenotype. Therefore, this project aimed to attempt different heat stress assays with the aim of discovering a phenotype in null mutants. Thus, I sought to find the optimal temperature that affects WT plants to set seeds and develop a seed setting heat stress assay to test on sHSP mutants. To limit variability, the heat stress was completed during the same time during each day (4 hrs into the 16 hr day cycle). However, it may reduce variability even more to heat stress the plants only one day rather than over two days. In addition, *hot1-3* plants were exposed to the same heat treatment. The *hot1-3* plants are null for the HSP101 mutant and are known to have significant phenotypes from heat stress. The WT plants heat treated at 34°C saw a slight reduction in fertility at the marked silique, however there was no reduced fertility seen in the *hot1-3* siliques at the same heat-treatment. This could indicate that the reduced fertility seen at the marked silique could have been caused by the tying of the thread rather than the heat stress condition. Additionally, the flowers were meant to be marked in the 12-13 development stage; however, the flowers were actually marked closer to early stage 15 of development. This could explain why there is no reduced fertility observed before the marked

silique and only after as it was already late into development. However, both WT and *hot1*-3 plants showed a reduced fertility in response to 38°C heat treatment. This shows that the optimal temperature to affect seed setting is 38°C. The next step would be to test the sHSP mutants with this heat stress protocol at 38°C over one day and to mark the siliques at an earlier development stage.

Future Directions

Creating an antibody that recognizes HSP23.5

The goal of the HSP23.5 antibody production was to acquire a tool to help investigate these sHSPs and their function to protect the plant during heat stress. The antibody will need to be tested for efficiency and specificity once it is produced. After the HSP23.5 antibody is tested, it can be used to confirm the HSP23.5 null mutant in the Vierling lab. As this is the only antibody for the four organelle sHSPs the Vierling lab did not have, the HSP23.5 mutant has not been confirmed. A western blot will need to be performed on *hsp23.5* with the HSP23.5 antibody and will hopefully result in no protein band. Another direction for this tool would be to test for sHSP compensation. In has been suggested that the downregulation or knockout of HSPs or sHSPs can lead to an upregulation of other sHSPs and of the ATP-dependent HSPs. It would be worthwhile to test the HSP23.5 amount in other sHSP mutants in the lab against WT amounts, as well as test the other sHSP antibodies or antibodies against other organelle-localized, or even cytosolic HSPs.

Creating CRISPR/cas9 HSP25.3 Mutant

Experiments were initiated to generate a new HSP25.3 mutant in the Columbia background as a future tool in the Vierling lab to investigate the function and properties of HSP25.3. However, it is of interest to also transform the construct into the *mtko* background or cross with the HSP25.3 Col mutant with *mtko* to create a new *qko*. The plants have been harvested for T1 seeds and screened with hygromycin antibiotics. Currently with the help of lab member Fabian Suri-Payer, around 30 T1 plants are growing and being genotyped. The next step is to harvest the T1 plants and begin screening the T2 seeds. Eventually, homozygous lines need to be identified and confirmed. Additionally, it is important to backcross the mutant to WT plants in order to remove the Cas9 gene. Cas9 can also generate off-target mutations and removing the gene from the mutant would eliminate any complications from the Cas9 protein. However, one concern with this mutant generation is the relatively large size of designed deletion (488 bp). Efficiency of this size deletion is unknown. It is possible that smaller or other deletions in the HSP25.3 gene may occur to create a null mutant other than the expected deletion. While these cannot be identified by simple differences in the size of PCR fragments amplified from the gene, they can be identified by sequencing of the PCR fragments. Once these mutants are confirmed, they can then be used to study further the sHSPs through different growth and stress assays.

HSP-GFP Localization

The localization of the HSP-GFP fusion lines lead to further questions. The HSP23.5 and HSP23.6 fusion lines showed clear expression at RT in both leaves and roots. Though it may be indicated for HSP23.5, this was not predicted from any database that there should be HSP23.6 expression at room temperature. Additionally, there was never clear localization seen in chloroplasts, even with the HSP25.3-GFP fusion lines where HSP25.3 is known to localize to the

chloroplast. Different heat stress treatments can be done prior to observing samples under the microscope. It maybe that the heat stress is causing protein aggregation or blocking transport. It would be interesting to see localization in these sHSP-GFP fusion lines at different heat treatments. Also, more lines could be observed under the same conditions to confirm the expression and localization further.

Generating Complementation vectors for the sHSP mutants

The complementation vectors have been generated and are currently in plasmid DNA stocks. However, only one of the complementation vectors, p1427, was confirmed through sequencing. The next step will be to further confirm the sHSP complementation vectors through sequencing and sequence alignments. This can be done by designing new primers to sequence the entire sHSP genes in the new plasmids. After the confirmation of the complementation vectors through sequencing, the constructs can be transformed into agrobacterium. Then the complementation vectors can be transformed into *A. thaliana* plants through floral dipping. The seeds would then need to be harvested and the screening process will need to be done to identify homozygotes for the reintroduced gene. Once the complementation vectors are transformed and homozygous plants are identified, the lines can be used in heat stress assays with the mutants. The complemented lines should behave like WT plants with the reintroduction of the sHSP genes and this will further prove a mutant phenotype is due to the null sHSPs.

Heat Stress Assays on sHSP mutants

More heat stress assays can be conducted on the sHSP mutants. First, the heat stress protocol for seed setting can be done on some of the organelle sHSP mutants to determine if there is a seed setting phenotype in any of the sHSP mutants. However, the heat stress treatments should occur over one day rather two to limit variability. It is recommended to attempt the assay at 38°C for 4 hrs and 6 hrs for one day. It would also be of note to mark the flowers before heat stress at an earlier stage (developmental stage 12-13) and to tie the thread carefully to reduce damage to the flower. Various other heat stress assays can be completed on the sHSP mutants such as root elongation assays, hypocotyl elongation assays, and much more. Literature can be reviewed to determine and develop new heat stress assays to perform on the sHSP mutants.

References

Basha, E., O'Neill, H., & Vierling, E. (2012). Small heat shock proteins and α-crystallins: Dynamic proteins with flexible functions. *Trends in Biochemical Sciences*, *37*(3), 106–117. https://doi.org/10.1016/j.tibs.2011.11.005

Cai, S., & Lashbrook, C. C. (2008). Stamen Abscission Zone Transcriptome Profiling Reveals New Candidates for Abscission Control: Enhanced Retention of Floral Organs in Transgenic Plants Overexpressing Arabidopsis ZINC FINGER PROTEIN2. *Plant Physiology*, *146*(3), 1305–1321. https://doi.org/10.1104/pp.107.110908

DeRocher, A. E., Helm, K. W., Lauzon, L. M., & Vierling, E. (1991). Expression of a Conserved Family of Cytoplasmic Low Molecular Weight Heat Shock Proteins during Heat Stress and Recovery 1. *Plant Physiology*, *96*(4), 1038–1047.

Harrison, S. J., Mott, E. K., Parsley, K., Aspinall, S., Gray, J. C., & Cottage, A. (2006). A rapid and robust method of identifying transformed Arabidopsis thaliana seedlings following floral dip transformation. *Plant Methods*, *2*(1), 19. https://doi.org/10.1186/1746-4811-2-19

Haslbeck, M., & Vierling, E. (2015). A First Line of Stress Defense: Small Heat Shock Proteins and their function in protein homeostasis. *Journal of Molecular Biology*, *427*(7), 1537–1548. https://doi.org/10.1016/j.jmb.2015.02.002

Heckathorn, S. A., Downs, C. A., Sharkey, T. D., & Coleman, J. S. (1998). The Small, Methionine-Rich Chloroplast Heat-Shock Protein Protects Photosystem II Electron Transport during Heat Stress. *Plant Physiology*, *116*(1), 439–444.

Hong, S.-W., & Vierling, E. (2001). Hsp101 is necessary for heat tolerance but dispensable for development and germination in the absence of stress. *The Plant Journal*, *27*(1), 25–35. https://doi.org/10.1046/j.1365-313x.2001.01066.x

Logan, D. C., & Leaver, C. J. (2000). Mitochondria-targeted GFP highlights the heterogeneity of mitochondrial shape, size and movement within living plant cells. *Journal of Experimental Botany*, *51*(346), 865–871.

Ma, W., Guan, X., Li, J., Pan, R., Wang, L., Liu, F., Ma, H., Zhu, S., Hu, J., Ruan, Y.-L., Chen, X., & Zhang, T. (2019). Mitochondrial small heat shock protein mediates seed germination via thermal sensing. *Proceedings of the National Academy of Sciences of the United States of America*, *116*(10), 4716–4721. https://doi.org/10.1073/pnas.1815790116

McLoughlin, F., Basha, E., Fowler, M. E., Kim, M., Bordowitz, J., Katiyar-Agarwal, S., & Vierling, E. (2016). Class I and II Small Heat Shock Proteins Together with HSP101 Protect Protein Translation Factors during Heat Stress1[OPEN]. *Plant Physiology*, *172*(2), 1221–1236. https://doi.org/10.1104/pp.16.00536

Prasad, P. V. V., Staggenborg, S. A., & Ristic, Z. (2008). Impacts of Drought and/or Heat Stress on Physiological, Developmental, Growth, and Yield Processes of Crop Plants. In *Response of Crops to Limited Water* (pp. 301–355). John Wiley & Sons, Ltd. https://doi.org/10.2134/advagricsystmodel1.c11

Sanmiya, K., Suzuki, K., Egawa, Y., & Shono, M. (2004). Mitochondrial small heat-shock protein enhances thermotolerance in tobacco plants. *FEBS Letters*, *557*(1–3), 265–268. https://doi.org/10.1016/S0014-5793(03)01494-7

Santhanagopalan, I., Basha, E., Ballard, K. N., Bopp, N. E., & Vierling, E. (2015). Model Chaperones: Small Heat Shock Proteins from Plants. The Big Book on Small Heat Shock Proteins (pp. 119–153).

Santhanagopalan, I., Degiacomi, M. T., Shepherd, D. A., Hochberg, G. K. A., Benesch, J. L. P., & Vierling, E. (2018). It takes a dimer to tango: Oligomeric small heat shock proteins dissociate to capture substrate. *The Journal of Biological Chemistry*, *293*(51), 19511–19521. https://doi.org/10.1074/jbc.RA118.005421

Siddique, M., Gernhard, S., von Koskull-Döring, P., Vierling, E., & Scharf, K.-D. (2008). The plant sHSP superfamily: Five new members in Arabidopsis thaliana with unexpected properties. *Cell Stress & Chaperones*, *13*(2), 183–197. https://doi.org/10.1007/s12192-008-0032-6

Thuiller, W. (2007). Climate change and the ecologist. *Nature*, *448*(7153), 550–552. https://doi.org/10.1038/448550a

Van Aken, O., Zhang, B., Carrie, C., Uggalla, V., Paynter, E., Giraud, E., & Whelan, J. (2009). Defining the Mitochondrial Stress Response in Arabidopsis thaliana. *Molecular Plant*, *2*(6), 1310–1324. https://doi.org/10.1093/mp/ssp053

Wang, Z.-P., Xing, H.-L., Dong, L., Zhang, H.-Y., Han, C.-Y., Wang, X.-C., & Chen, Q.-J. (2015). Egg cell-specific promoter-controlled CRISPR/Cas9 efficiently generates homozygous mutants for multiple target genes in Arabidopsis in a single generation. *Genome Biology*, *16*(1). https://doi.org/10.1186/s13059-015-0715-0

Waters, E. R., & Vierling, E. (1999). Chloroplast small heat shock proteins: Evidence for atypical evolution of an organelle-localized protein. *Proceedings of the National Academy of Sciences*, *96*(25), 14394–14399. https://doi.org/10.1073/pnas.96.25.14394

Waters, E. R., & Vierling, E. (2020). Plant small heat shock proteins – evolutionary and functional diversity. *New Phytologist*, *227*(1), 24–37. https://doi.org/10.1111/nph.16536

Waters, E. R., Lee, G. J., & Vierling, E. (1996). Evolution, structure and function of the small heat shock proteins in plants. *Journal of Experimental Botany*, *47*(3), 325–338. https://doi.org/10.1093/jxb/47.3.325

Xing, Hui-Li, et al. "A CRISPR/Cas9 Toolkit for Multiplex Genome Editing in Plants." *BMC Plant Biology*, vol. 14, no. 1, Nov. 2014, p. 327. *BioMed Central*, doi:10.1186/s12870-014-0327-y.

Zhong, L., Zhou, W., Wang, H., Ding, S., Lu, Q., Wen, X., Peng, L., Zhang, L., & Lu, C. (2013). Chloroplast Small Heat Shock Protein HSP21 Interacts with Plastid Nucleoid Protein pTAC5 and Is Essential for Chloroplast Development in Arabidopsis under Heat Stress. *The Plant Cell*, *25*(8), 2925–2943. https://doi.org/10.1105/tpc.113.111229

Appendix:

Appendix Table 1. A list of primers, their function, and their sequence in the 3' to 5' direction

Primer Name	Function/Description	Sequence 5'-3'
357	U6-26p-F, to screen for CRISPR-Cas9 plasmid pHEE/C-401 with gRNA	TGTCCCAGGATTAGAATGATTAGGC
358	U6-29p-R, U6-26p-F + U6-29p-R = 726 bp	AGCCCTCTTCTTTCGATCCATCAAC
444	to clone any insert into p1000 in frame to generate HIS-SUMO tagged proteins, rev	ACCACCGGTCTGTTCTCTGTG
445	to clone any insert into p1000 in frame to generate HIS-SUMO tagged proteins, fwd.	CGAGCACCACCACCACCACCACTG
475	Forward subcloning HSP truncation for Antibody prod. of p1405.	CAGAGAACAGACCGGTGGTTTCAATACCAAC GCCGCCAG
476	Reverse subcloning HSP truncation for Antibody prod. of p1405.	GGTGGTGGTGGTGGTGCTCGCTAGATTTCGCT TACCTGGTCC
477	DT1-BsF (to generate 2 gRNA CRISPR USING Golden Gate Cloning (HSP25.3))	ATATATGGTCTCGATTGCTACACCGTTCTCGGTTTC GGTT
478	DT1-F0 (to generate 2 gRNA CRISPR USING Golden Gate Cloning (HSP25.3))	TGCTACACCGTTCTCGGTTTCGGTTTTAGAGCTAG AAATAGC
479	DT2-R0 (to generate 2 gRNA CRISPR USING Golden Gate Cloning (HSP25.3))	AACCTTTGATGTCCCACGGTGCACAATCTCTTAGT CGACTCTAC
480	DT2-BsR (to generate 2 gRNA CRISPR USING Golden Gate Cloning (HSP25.3))	ATTATTGGTCTCGAAACCTTTGATGTCCCACGGTG CACAA

495	To generate HSP23.5 complementation construct from plasmid PP5	CCAAAATAAAACACTCTAGTCAACGTTTATGTGACGAATATTG
496	To generate HSP23.5 complementation construct from plasmid PP5	GTTCGTGTCGGCATCGTCAGATCGGGAATTCG
497	To generate HSP23.5 complementation construct from genomic DNA	CAATATTCGTCACATAAACGTTGACTAGAGTGTTTTATTTTGG
498	To generate HSP23.5 complementation construct from genomic DNA	CGAATTCCCGATCTGACGATGCCGACACGAACGAGT
517	Forward DNA insert primer to generate HSP23.6 Complementation vector from PP6	CAGATCGAGATCAACTAAAAACGTCGACG
518	Reverse Backbone primer to generate HSP23.6 complementation vector from PP6	CGTCGACGTTTTTAGTTGATCTCGATCTG
519	Forward Backbone primer to generate HSP23.6 complementation vector from PP6	GTCGACGGACTGGTCTAGATCGGGAATTCGTAATC
520	Reverse DNA insert primer to generate HSP23.6 Complementation vector from PP6	GATTACGAATTCCCGATCTAGACCAGTCCGTCGAC
521	Forward DNA insert primer to generate HSP25.3 Complementation vector from PP7	GATGTCCAGATTCAGTAGGACTCGATCAAC
522	Reverse Backbone primer to generate HSP25.3 complementation vector from PP7	GTTGATCGAGTCCTACTGAATCTGGACATC
523	Forward Backbone primer to generate HSP25.3 complementation vector from PP7	CGTTCATAAGATATGAGATCGGGAATTCG
524	Reverse DNA insert primer to generate HSP25.3 Complementation vector from PP7	CGAATTCCCGATCTCATATCTTATGAACG
525	Forward DNA insert primer to generate HSP26.5 Complementation vector from PP8	CAGGAGATTTCTGTTGAGTAGAAGAGATACGGTG
526	Reverse Backbone primer to generate HSP26.5 complementation vector from PP8	CACCGTATCTCTTCTACTCAACAGAAATCTCCTG
527	Forward Backbone primer to generate HSP26.5 complementation vector from PP8	CTTTTAGTTTGGTATTAGATCGGGAATTCGTAATC
528	Reverse DNA insert primer to generate HSP26.5 Complementation vector from PP8	GATTACGAATTCCCGATCTAATACCAAACTAAAAG
565	Forward Primer to amplify Hsp23.6 (AT4G25200) to create p1426	TAAaaacgtcgacgttttttc
566	Reverse Primer to amplify Hsp23.6 (AT4G25200) to create p1426	agaccagtccgtcgacaactt
567	Forward Primer to amplify Hsp25.3 (AT4G27670) to create p1427	TAGgactcgatcaacattatcctc
568	Reverse Primer to amplify Hsp25.3 (AT4G27670) to create p1427	catatcttatgaacgattcc
569	Forward Primer to amplify Hsp26.5 (AT1G52560) to create p1428	TAGaagagatacggtgtcgtttttg
570	Reverse Primer to amplify Hsp26.5 (AT1G52560) to create p1428	aataccaaactaaaagaagg
ISOKAN1	to generate fragments for Gibson assembly on vectors that contain kanamycin resistance	GCCTGTTCCAAAGGTCCTGCACTTTG
ISOKAN2	to generate fragments for Gibson assembly on vectors that contain kanamycin resistance	CAAAGTGCAGGACCTTTGGAACAGGC

Appendix Table 2. A list of plasmid names and a description.

Number	Name	Description
p1384	pHEE401E	Plant Expression, CRISPR ; Plant binary vector, Z.m. codon optimized Cas9 protein with 3x n-terminal Flag tag and SV40 NLS. Under control of embryo specific promotor and enhancer
p1385	pCBC-DT1T2	Plant Expression, CRISPR ; PCR template
p1405	pET23b-HIS-SUMO-HSP23.5	(GA cloning) Subcloning of HSP23.5 into HIS-SUMO construct (initial construct is non tagged) for IMAC purification and subsequent cleavage of the HIS-SUMO tag, no starting Met
P1416	pET23b-HIS-SUMO-truncHSP23.5	GA cloning of p1405 to generate a truncated HSP protein for antibody production
p1417	pHEE401E-HSP25.3	Golden gate assembly: 2 guide RNAs to generate CRISPR knockouts of HSP25.3 using primers 477-480
p1425	PP5-HSP23.5modified	complementation construct encoding HSP23.5 genomic region, including promotor, 5 and 3´UTR and "terminator region"
p1426	PP6-HSP23.6 modified	complementation construct encoding HSP23.6 genomic region, including promotor, 5 and 3´UTR and "terminator region"
p1427	PP7-HSP25.3 modified	complementation construct encoding HSP25.3 genomic region, including promotor, 5 and 3´UTR and "terminator region"
p1428	PP8-HSP26.5 modified	complementation construct encoding HSP25.3 genomic region, including promotor, 5 and 3´UTR and "terminator region"

```
# Identity:      84/111 (75.7%)
# Similarity:    97/111 (87.4%)
# Gaps:           2/111 ( 1.8%)
# Score: 423


ΔN-HSP23.5          1 MGASGVRRGWNVKEKDDALHLRIDMPGLSREDVKLALEQNTLVIRGEGET     50
                      |||||.||||::|||||||:||||||||||||||||||:||||||||:.
ΔN-HSP23.6          1 MGASGARRGWDIKEKDDALYLRIDMPGLSREDVKLALEQDTLVIRGEGKN     50

ΔN-HSP23.5         51 EE--GEDVSGDGRRFTSRIELPEKVYKTDEIKAEMKNGVLKVVIPKIKED     98
                        ||  ||:.....|||||||.||:|:||.||||||||||||||||:||.
ΔN-HSP23.6         51 EEDGGEEGESGNRRFTSRIGLPDKIYKIDEIKAEMKNGVLKVVIPKMKEQ    100

ΔN-HSP23.5         99 ERNNIRHINVD    109
                        |||::|.|.::
ΔN-HSP23.6        101 ERNDVRQIEIN    111
```

Appendix Figure 1: Protein Sequence alignment of the ACD and NTD of HSP23.5 and HSP23.6. The most highly conserved domains (ACD and NTD) were compared in a sequence alignment between HSP23.5 and HSP23.6 comparing amino acid 108 to 210. properties, and two dots represent strongly similar properties. No dot represents no relationship. Alignments were executed using Pairwise Sequence Alignment software. The Emboss Matcher program was used under Pair format.

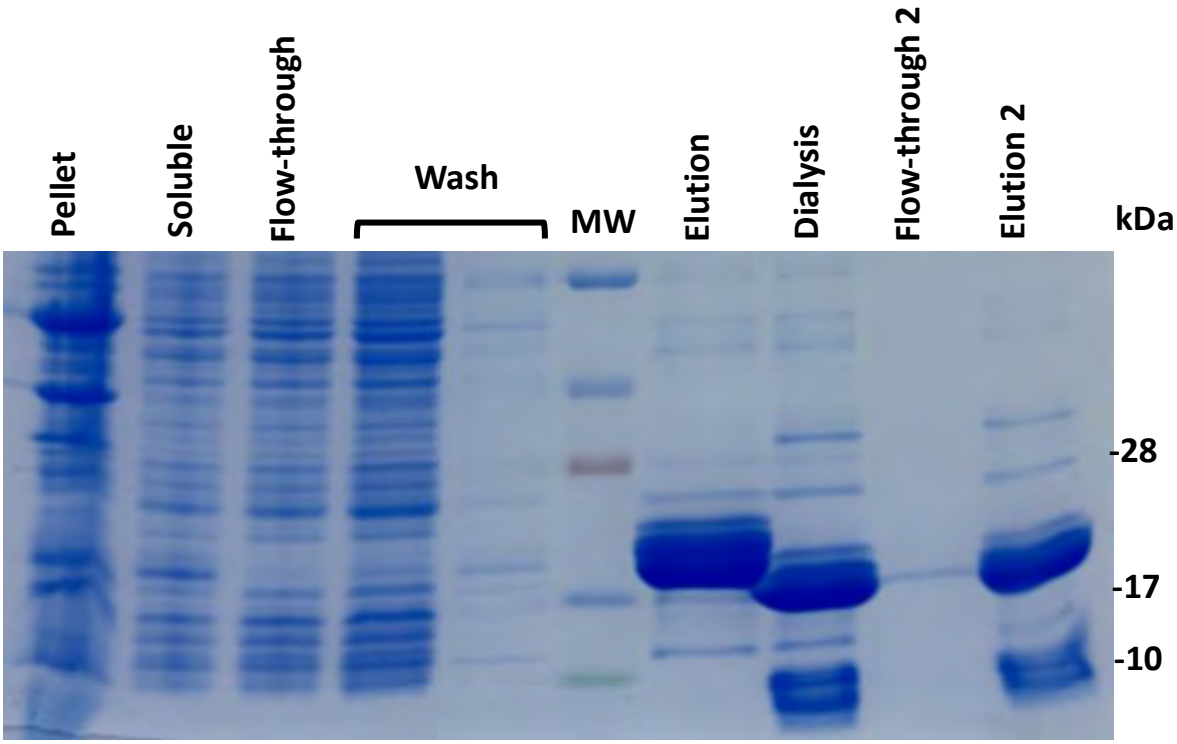

Appendix Figure 2: Initial Purification and Cleavage Attempt of ΔC-Hsp23.5 using FPLC and a Nickel Resin. The lanes pellet, soluble, Flow-through, Wash, Elution, dialysis, flow-through 2, and elution 2 represent fractions collected during the purification attempt. The cells expressing ΔC-Hsp23.5 were pelleted, then resuspended in lysis buffer and disrupted with a microfluidizer. The solution was centrifuged down. The samples of the supernatant (soluble) and pellet were taken. The supernatant was run through a nickel resin with an FPLC machine and the flow-through was collected. The column was washed with lysis buffer. And then eluted with elution buffer. The elution fraction was set up in a dialysis against 1x PBS and the His-SUMO tag was cleaved with an ULP1 protease (dialysis). The sample was then loaded back onto the nickel column and the flow through was collected (flowthrough 2). The column was eluted with elution buffer (elution 2). The tagged, truncated protein was expected to be 18.95 kDa. The cleaved truncated protein is expected to be 6.61 kDa. The cleaved tag is expected to be 12.34 kDa.

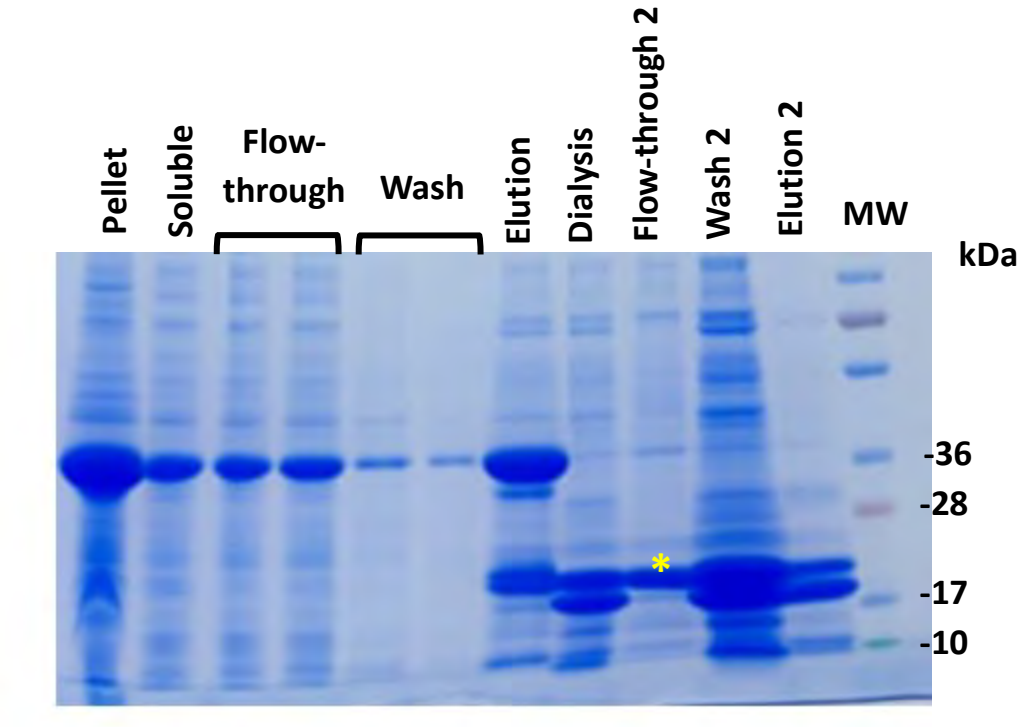

Appendix Figure 3: Purification and Cleavage of Hsp23.5 using FPLC and a Nickel Resin. The lanes pellet, Soluble, Flow-through, Wash, Elution, Dialysis, Flow-through 2, Wash 2, and Elution 2 represent samples from the purification fractions. The cells expressing ΔC-Hsp23.5 were pelleted, then resuspended in lysis buffer and disrupted with a microfluidizer. The solution was centrifuged down. The samples of the supernatant (soluble) and pellet were taken. The supernatant was run through a nickel resin with an FPLC machine and the flow-through was collected. The column was washed with lysis buffer. And then eluted with elution buffer. The elution fraction was set up in a dialysis against 1x PBS and the His-SUMO tag was cleaved with an ULP1 protease (Dialysis). The tag and cleaved full-length protein were then loaded onto the column (flowthrough 2) and washed with 1x PBS (wash 2). The column was then eluted with elution buffer (Elution 2). The tagged, HSP23.5 protein was expected to be 32.1 kDa. The cleaved full-length protein is expected to be 19.8 kDa. The cleaved tag is expected to be 12.34 kDa. The yellow asterisk indicates the Hsp23.5 protein at 19.8 kDa.